Department of Chemical Engineering

Modelling Immiscible Liquid-Liquid Dispersion by Population Balance Equation

by

YANG YANG

(ID:B118102)

A master's course dissertation

Submitted in partial fulfilment of the requirements for the award of

Master of Science in Advanced Chemical Engineering with Information Technology & Management Engineering

August 2013

Acknowledgements

I would like to express my great appreciation to my supervisor Professor Chris D. Rielly for his patient guidance, enthusiastic encouragement and valuable critiques of this research work. No matter how busy he was in the last year, an inspiring meeting was arranged every week. Without his useful and constructive recommendations, this project is impossible to be completed.

I would also like to thank to Dr. Karen Coopman for her instruction and help during my study.

My grateful thanks are also extended to Miss Anna Temple, Miss Yasmin Kosar and all the staff of Department Chemical Engineering at Loughborough University for their help on finishing this project.

Finally, I wish to thank my parents for their love and encouragement in all my life.

Executive Summary

Multi-phase mixing is a major problem in several industries application as it involves mass and heat transfer as well as the rate of the chemical reaction. Generally, the mechanism of mixing process is not completely understood due to the complexity of the phenomena existing during the mixing. In the past decades, intensive models have been developed to explain and simulate the multi-phase mixing process. Particularly for gas-liquid dispersion, massive effort has been devoted into the investigation of the phenomena modelling such as breakage, coalescence, nucleation, growth and aggregation during the mixing, but little work has been done on the description of the overall immiscible liquid-liquid dispersion. Recently, population balance equation(PBE) solved by the quadrature method of moments(QMOM) has become a very popular method for describing process of multi-phase mixing, so it has been employed to analyse the immiscible liquid-liquid dispersion in this project. The work has shown detail about how droplet data in a liquid-liquid system has been acquired in order to analyse the transition of the droplet size distribution. The 0^{th}~5^{th} moments have been calculated by QMOM for testing the validation of the proposed models. The transient Sauter mean diameter is predicated with analysis of several different physical factors.

The dissertation mainly contains four chapters. Chapter one briefly introduces the concepts of the immiscible liquid-liquid system. Chapter two reviews the fundamental knowledge about the PBE and Chapter three presents all the experimental information, methods and results discussion in format of manuscript for publication in *Chemical Engineering Journal*. The last chapter summarizes the report with a conclusion and recommendation, project definition & plan, minutes and work for the MSc project.

TABLE OF CONTENTS

List of Figures and Tables

Nomenclature

$A(V,t)$	number fraction for the drops of volume V at time t
$C_1, C_{2,} C_3, C_{4,} C_5$	experimental constants
D	drop diameter(m)
$\overline{D}$	mean drop diameter (m)
D_I	impeller diameter(m)
$\overline{E}$	mean turbulent kinetic energy (dynes-cm)
E_s	surface energy of drops(dynes-cm)
F	force per unit mass acting on a droplet(N/kg)
$g(V)$ $g(D)$	breakage frequency of drops of volume V and of diameter D, respectively (s^{-1})
$h(V,V_1)$	coalescence efficiency
k	numerical constant
L_T	turbulent macro length scale (m)
$m(V)$	number of daughter drops of volume V
M_{crit}	critical mass of drop that can breakup(kg)
M_{max}	maximum mass of drop(kg)
$n(D,x,t)$	number of drops of size D at specific position x at time t
$n(V,t)$	number of drops of volume V at time t
$N(t)$	total number of drops at time t
N_I	diameter of impeller (m)
$p(D,x,\nu,t)$	number of droplets of size D at spatial position x with velocity ν at time t
$\dot{Q_b}$	number changed by breakage under uniform velocity (s^{-1})
$\dot{Q_c}$	number changed by coalescence under uniform velocity(s^{-1})
$\dot{Q_b}$	number changed by breakage(s^{-1})
$\dot{Q_c}$	number changed by coalescence (s^{-1})
$r(V)$	variable
R	number of droplets size D changed due to the evaporation, condensation or dissolution(s^{-1})
Re	Reynolds number of stirred vessel

t	time(s)
V_1	Volume of drop
V_{max}	maximum volume of drop
We	Weber number
x	specific spatial position on axial

Greek Symbols

$\beta(V, V_1)$	frequency of daughter drops of volume V resulting from breakage of parent drops of volume V_1
δ	standard deviation
ϵ	local energy dissipation rate per mass of fluid(W/kg)
$\bar{\epsilon}$	average energy dissipation rate per mass of fluid(W/kg)
ζ	numerical constant
η	Kolmogoroff microscale of turbulence(m)
$\lambda(V, V_1)$	Collision frequency between drops of volume V and V_1
$\bar{\mu}$	mean viscosity of mixing phase(Pa·s)
μ_c	viscosity of continuous phase(Pa·s)
ρ_c	density of continuous phases (kg/m^3)
ρ_d	density of dispersed phases (kg/m^3)
$\bar{\rho}$	mean density of mixing phase (kg/m^3)
τ_b	breakage time(s)
ν_c	kinematic viscosity of continuous phase (m^2/s)
ϕ	volume fraction of dispersed

Chapter 1

1.1. Description of The Project

The project mainly focuses on the investigation of liquid-liquid dispersion, usually water and organic solvent. Since the information such droplet size distribution of the droplet, plays a key role for industrial application, it is essential to require the detail during the blending and this is exactly what the project expects.

First of all, a primary literature survey reviews the current situation of the population balance equation (PBE) and relevant models required to close the population balance equation. Secondly, some program codes for solving the PBE and are developed in software MATLAB. Then, the model is tested in parameter fitting procedure by analysing against the droplet size measurement from a dense liquid-liquid dispersion, where is assumed fully turbulent. The experimental data is obtained from an on-line work done by Sebastian Maab (2012). Finally, the model is deployed to simulate the transient Sauter mean diameter which is a key figure for describing the dynamic process. The model developed in this project presents some reasonably good results on some aspects.

In order to improve the accuracy of the predicated results, the model should be modified to predict inhomogeneity occurring in the stirred tank. The local energy dissipation rate needs to be obtained from the experiment to replace the average energy dissipation rate used for the simulation results. The impact such as the height of the liquid, length of the baffles, type of impellers on the final Sauter mean diameter is advised to investigate for the future work.

Chapter 2

2.1. A Brief Literature Survey

2.1.1. Introduction

System of two immiscible liquids commonly exists in the chemical, mining, petroleum and pharmaceutical industries, nevertheless it is one of the most challenging and least understand cases for two-phase mixing process. Insufficient description for the mixing process may cause inappropriate designing for liquid-liquid reactors, stirred vessels and extraction columns. Although extensive empiricism correlations have been developed and applied in the previous work, some limitations have appeared if more detailed hydrodynamic information is required such as droplets size distribution (DSD) or they are supposed to be applied under more complex operation conditions where some parameters might not be applicable or safety margins possibly are hard to meet the requirement. Thus, large amount of pilot scale tests are necessary and it may incur extra cost of budget and time. Population Balance Equation (PBE), a mathematical tool emerged as a more reliable, accurate and sophisticated method to simulate dynamic behaviour for immiscible liquid-liquid dispersion and provide accurate results.

Immiscible liquid-liquid dispersion refers to two completely immiscible liquids mixing in an agitated vessel where two separate phases can be observed clearly. Generally, the phase of smaller volume fraction is referred as the dispersed phase and the other is considered as continuous phase. The interfacial area between two phases is a key parameter having great influence on the rate of mass transfer and chemical reaction. It is normally related to the drop size, so it would be better to oblation a detailed description of droplets size in the agitated vessel.

Compared with empirical methods, PBE has advantage of showing precise information of droplets size distribution. It is also able to predicate DSD in a stirred vessel when appropriate models are employed. At present, it has been accepted as the most powerful and flexible approach for modelling multi-phase mixing process. Nevertheless, it is not a completely perfect method, as it contains many integral-differential equations. Sometimes analytical solution is not available, so large amount

of computing caused in development of appropriate solution for the equation is inevitable.

2.1.2. Population balance equation

Population balance modelling basically is based on mass balance. Similarly, a control volume is required such as a stirred tank where two liquids are well mixed. To simplify the system, it assumes that no liquid flowing in and out. Then, some differential equations with droplets size or droplets volume as internal coordinate are created to indicate the information such as breakage frequency, daughter size distribution, coalescence efficiency and collision frequency (Marchisio et al.,2003). A general population balance equation is written as follow (Williams,1985):

$$\frac{\partial n(D,x,t)}{\partial t} = \dot{Q_b} + \dot{Q_c} \tag{2.1.1}$$

where $n(D,x,t)$ means the number of droplets within the specific position x at time t, $\dot{Q_b}$ and $\dot{Q_c}$ represent phenomena of breakage and coalescence respectively.

In a stirred vessel, physical properties may vary from one point to another such as densities, viscosities and interfacial tension, because the composition of the dispersed phase and continuous phase is not uniform. In addition, the energy dissipation rate within the impeller regions obviously is much higher than anywhere else. These factors increase the difficulty of modelling by PBE. To simplify the system the investigation only focuses on the high turbulent flow reign and assumes the system is well mixed.

In a highly turbulent agitated vessel where Reynolds number Re is defined as:

$$Re = \frac{D_I^2 N_I \bar{\rho}}{\bar{\mu}} \tag{2.1.2}$$

D_I and N_I are the impeller diameter and speed, respectively. $\bar{\rho}$ and $\bar{\mu}$ refer to the average density and viscosity of the system, respectively (Paul et al, 2004). The system can be regarded as homogeneous if $Re > 10^4$. Therefore, it is reasonable to make the assumption the system is ideally uniform.

According to Coulaloglou and Tavlarides (1977), $n(D,t)$ is also expressed as:

$$n(V,t) = N(t)A(V,t) \tag{2.1.3}$$

where $N(t)$ is the total number of drops in the vessel at time t, and $A(V,t)$ is normalised number fraction for the drops of volume V which is related to D by $V \sim D^3$. The total number of the droplets are reduced and increased by mechanism such as breakage, coalescence, nucleation and evaporation in the system. For immiscible liquid mixing, breakage and coalescence are the major factors affecting variation of the number of the droplets and other impacts are neglected.

Breakage term $\dot{Q}_b$ is expended as:

$$\dot{Q}_b = \int_V^{V_{max}} \beta(V_1, V)\, m(V_1) g(V_1) N(t) A(V_1, t) dV_1 - g(V) N(t) A(V, t) \tag{2.1.4}$$

where $\beta(V_1, V)$ means the distribution of daughter drops of size V formed from the breakage of a parent drop of size V_1. $m(V_1)$ refers to the possible number of daughter drops formed from breakage of a mother drop of size V_1. Breakage frequency for a drop of size V_1 is denoted by $g(V_1)$.Thus, the terms on the right hand side mean the rate of formation and loss of drops of size V due to the breakage.

Similarly, coalescence term $\dot{Q}_c$ is expressed as

$$\dot{Q}_c = \int_0^{\frac{V}{2}} \lambda\,(V - V_1, V_1) h(V - V_1, V_1) N(t) A(V - V_1, t) N(t) A(V_1, t) dV_1 - N(t) A(V, t) \times \int_0^{V_{max} - V} \lambda(V, V_1) h(V, V_1) N(t) A(V_1, t) d\,V_1 \tag{2.1.5}$$

where $\lambda(V - V_1, V_1)$ is the collision frequency of the droplets of volume of $V - V_1$ with drops of volume V_1; $h(V - V_1, V_1)$ means the coalescence efficiency between drops of volume $V - V_1$ and drops of volume V_1. Normally, two droplets coalesce into one and the chance for more than two droplets coalesce into one is negligible (Lasheras et al. 2002). The first term on the right hand side indicates the formation of two drops with volume of $V - V_1$ and V_1. It is necessary to define that $(V - V_1) \geq V_1$ to avoid counting contribution twice from the same pair of drops, so the upper limit sets as $\frac{V}{2}$ (Valentas and Amundson, 1966). The second term on the right hand side means the loss of the drops of size V by coalescing with drops of all other size.

Substituting Eq. (2.1.3), (2.1.4) and (2.1.5) into (2.1.1), a general population balance is converted into:

$$\frac{\partial}{\partial t}N(t)A(V,t) = \int_{V}^{V_{max}} \beta(V_1,V)\, m(V_1)g(V_1)N(t)A(V_1,t)dV_1 - g(V)N(t)A(V,t) + \int_{o}^{\frac{V}{2}} \lambda\,(V-V_1,V_1)h(V-V_1,V_1)N(t)A(V-V_1,t)N(t)A(V_1,t)dV_1 - N(t)A(V,t) \times \int_{0}^{V_{max}-V} \lambda(V,V_1)h(V,V_1)N(t)A(V_1,t)d\,V_1 \qquad (2.1.6)$$

At steady state, time is avoided so eq. (8) is rearranged as:

$$NA(V) = \left[\int_{V}^{V_{max}} \beta(V_1,V)\, m(V_1)g(V_1)NA(V_1,t)dV_1 + \int_{o}^{\frac{V}{2}} \lambda\,(V-V_1,V_1)h(V-V_1,V_1)NA(V-V_1,t)NA(V_1,t)dV_1\right] / (g(V)+r(V)) \qquad (2.1.7)$$

Where $r(V) = \int_{0}^{V_{max}-V} \lambda(V,V_1)h(V,V_1)NA(V_1)d\,V_1$

Number fraction $A(V)$ is possible measured by experiment to generate real size distributions. Theatrical evolution of the drops size is simulated by fitting different models to the terms on the left hand side of the Eq. (2.1.7). Then, the validity of the PBE is tested by comparing the simulated results with the measured data. A numeric solution sometimes may be applied, because the analytical solution is not always applicable for complicated integral –differential equations.

2.1.3. Breakage Models

A spherical droplet in an agitated vessel is affected by internal viscous force, interfacial tension force and external mechanical forces (Paul et al 2004). In general, the external mechanical forces could be any fluid dynamical forces causing deformation to the droplet. The forces are resisted by the interfacial tension force and the internal viscous force. The droplet will not break unless the degree of deformation exceeds a critical value indicated by Weber number:

$$We = \rho N_I{}^2 D^3/\sigma \qquad (2.1.8)$$

Sometimes a droplet has been changed massively from the original spherical shape but it is still stable and unbroken, because internal circulation stabilizes the drop (Lasheras et al.,2002). Once breakage happens, a larger drop referred to as a parent drop splits into several smaller drops called daughter drops, the number of

which can be two called binary breakage or more than two called multiple breakage (Marchetti and Svendsen,2012). It is important to know the possible number of drops resulting from the breakage in order to predicting the overall droplets size distribution. In most cases, for simplifying breakage model, it is assumed that a parent drop only splits into two daughter droplets (Marchetti and Svendsen,2012;Coulaloglou and Tavlarides,1977;Valents et al, 1966). In fact, it is very rare to observe the binary breakage, especially for a possible case that two daughter drops are of the same size (Rumscheidt and Mason, 1961). Normally, droplets of various sizes are formed, so both size distribution of daughter droplets and breakage model are random events.

For breakage process, most models are built according to the collision between droplets and micro scale eddy. According to description by Shinnar (1961), a droplet is possible to break by collision with micro turbulences eddy of the same size. The micro turbulences eddy is first introduced by Kolmogoroff (1941).

Among the existing models, a phenomenological model developed by Coulaloglou and Tavlarides (1977) is most widely used. They related fraction of breaking drops to the ratio of surface energy to kinetic energy by

$$\frac{\Delta N(D)}{N(D)} = \exp(-\frac{E_s}{\overline{E}}), \tag{2.1.9}$$

where as $\overline{E} = C_2 \rho \epsilon^{\frac{2}{3}} D^{\frac{11}{3}}$ means turbulent kinetic energy and $E_s = C_3 \sigma D^2$ means surface energy of droplets. The estimation of the equation are based on the Kolmogoroff's theory (Kolmogoroff, 1941), by which D is assumed to within the inertial range: $L_T \gg D \gg \eta$. L_T is turbulent macro length scale and η is called Kolmogorov micro scale of turbulence defined as:

$$\eta = (\frac{\upsilon_c}{\epsilon})^{\frac{1}{4}} \tag{2.1.10}$$

where υ_c is kinematic viscosity of continuous phase.

They also defined breakage time τ_b:

$$\tau_b = C_3 D^{\frac{2}{3}} \epsilon^{-\frac{1}{3}} \tag{2.1.11}$$

where ϵ refers to local energy dissipation rate and is related to the physical properties of the impeller speed and diameter by $\epsilon \sim N_I^{\,3} D_I^{\,2}$.

Breakage frequency of a drop of size D is defined as:

$$g(D) = \frac{1}{\tau_b}\frac{\Delta N(D)}{N(D)} = \frac{1}{\tau_b}\exp\left(-\frac{E_s}{\bar{E}}\right), \tag{2.1.12}$$

which is rearranged and written as:

$$g(D) = C_4 D^{-2/3}\epsilon^{1/3}\exp\left(-\frac{C_5\sigma}{\rho\epsilon^{2/3}D^{5/3}}\right) \tag{2.1.13}$$

where C_4 and C_5 are constants determined by fitting measured data. An obvious drawback criticized later by Tsouris and Tavlarides (1994) is that the behaviour of the function is non-monotonic with droplet size. It means breakage frequency reaches highest value as the drop diameter raises to a critical drop diameter then it goes down slightly. It was pointed out to be not physically realistic (Chen, 1997;Lasheras et al 2002). Moreover, the surface energy depends only on the interfacial tension ignoring the impact of the viscous forces (Chen, 1997). An obvious mathematical error is also identified and revised in the work by Hsia and Tavlarides(1983).The final form is written as:

$$g(D_i) = C_1\frac{\varepsilon^{1/3}}{D_i^{2/3}(1+\phi)} \times \exp\left[-C_2\frac{\sigma(1+\phi)^2}{\rho_d\varepsilon^{2/3}D_i^{5/3}}\right] \tag{2.1.14}$$

Prince and Blanch (1990) and Konno (1980) postulated very similar models by showing monotonic behaviour with low energy dissipation rate, but it presents very similar result with models proposed by Coulaloglou and Tavlarides(1977) at high energy dissipation rate. It is also proved that the equation depended much on the integrating limit without providing a reasonable explanation (Lasheras et al.,2002). Luo and Svendsen(1996) proposed their kinetic models which also show great dependent on limits of integration, but they avoided any experimental constants. A simple summary of several models for breakage rate is shown in Table 1 (Marchetti and Svendsen, 2012).

Table 2.1.1. A brief summary of breakage frequency $g(D)$.

References	Mathematical Expression
Coulaloglou and Tavlarides(1977)	$g(D) = C_4 D^{-2/3} \epsilon^{1/3} \exp(-\frac{C_5 \sigma}{\rho \epsilon^{2/3} D^{5/3}})$
Konno (1980)	$g(D) = C_K \frac{\sqrt{\overline{\Delta U^2}(D)}}{D} \int_{U^*}^{\infty} 3\sqrt{\frac{6}{\pi}} \exp(-\frac{3x^2}{2})\, dx$ $U^* = U_c / \sqrt{\overline{\Delta U^2}(D)}, U \textit{ means the velocity of the droplet}$
Prince and Blanch (1990)	$g(D) = \int_0^{\frac{10\pi}{D}} \frac{0.14\pi}{16} \left(D + \left(\frac{2\pi}{K}\right)^2\right) \left(D^{\frac{2}{3}} + \left(\frac{2\pi}{K}\right)^{\frac{2}{3}}\right)^{\frac{1}{2}} \epsilon^{\frac{1}{3}} \times \exp(-\frac{1.18}{(2\pi)^{2/3}} \frac{\sigma K^{2/3}}{\rho D \epsilon^{3/3}}) K^2 dK$
Luo and Svendsen(1996)	$g(D; D_1) = 0.923(1-\phi) \left(\frac{\epsilon}{D^2}\right)^{\frac{1}{3}} \times \int_{\xi_{min}}^{1} \frac{(1+\xi)^2}{\xi^{11/3}} \exp(-\frac{12 C_f \sigma}{\beta \rho \epsilon^{2/3} D^{5/3} \xi^{11/3}}) d\xi$ $\xi = \frac{D_e}{D};\ \xi_{min} = \frac{D_{e,min}}{D};\ \frac{D_{e,min}}{\eta} = 11.4 \sim 31.4$ D_e means the diameter of the eddy.

2.1.4. Fragment Distribution Functions

Fragment distribution functions refer to some mathematical expressions associated with distribution of the daughter size. Only with the breakage frequency, is it impossible to complete a population balance. The distribution of the daughter size term $\beta(D_1, D)$ and the number of daughter drops resulted from breakage of a parent drop with size D_1, represented as $m(D_1)$ also need to be identified. In general, the number of daughter drops is given by assumed constants or deriving from the empirical equation. Two cases are proposed by Valents et al (1966). One is binary breakage with the formation of equal-sized daughter drops also called as discrete breakage kernel and the other is considering that a distribution of possible daughter

sizes could be formed (Valentas et al. 1966; Marchetti and Svendsen,2012). For later case, $\beta(D_1, D)$ was given by Valentas as a normal density function:

$$\beta(D_1, D) = \frac{1}{\delta\sqrt{2\pi}} \exp(-\frac{(D-\overline{D})^2}{2\delta^2}), \tag{2.1.15}$$

where D_1 means diameter of a parent drop relating to volume V_1 by $D_1 \sim V_1^{1/3}$. $\overline{D}$ is a mean value or expected value of D defined by

$$\overline{D} = \frac{D_1}{m(D_1)^{1/3}} \tag{2.1.16}$$

If D lies in a range specified by tolerance ζ of $\overline{D}$ expressed as $\overline{D} - \zeta \ll D \ll \overline{D} + \zeta$, then standard deviation δ is defined as,

$$\delta = \frac{D_1}{\zeta m(D_1)^{\frac{1}{3}}} \tag{2.1.17}$$

The result depends on the function $m(D_1)$, which is determined from experimental data. Table 2.1.2 shows some daughter size distribution functions provided by Coulaloglou and Tavlarides (1977), Hisa & Tavlarides(1983), Hesketh et al.(1991) and Martinez-Basan et al(1999). Among these functions, one proposed by Hisa and Tavlarides is mostly used and it is relative simple to implement with high accuracy.

Talbe 2.1.2. A brief summary of breakage kernels

References	**Mathematical Expression**
Coulaloglou & Tavlarides(1977)	$\beta(D^3, D_1^3) = \frac{2.4}{D_1^3} \exp(-\frac{-4.5(2D^3 - D_1^3)^2}{D_1^6}$
Hsia & Tavlarides(1983)	$\beta(D^3, D_1^3) = \frac{30}{D_1^3}\left(\frac{D^3}{D_1^3}\right)^2 (1 - \frac{D^3}{D_1^3})^2$
Hesketh et al.(1991)	$\beta(D^3, D_1^3) = \left(\frac{1}{B+\left(\frac{D}{D_1}\right)^3} + \frac{1}{\left(1+B-\left(\frac{D}{D_1}\right)^3\right)} - \frac{2}{B+0.5}\right)\frac{I}{D_1^3}$ I, B are constants

Although, equations or approaches employed to obtain the kernels are varied from one to another, the shape of the daughter drop size distributions can be divided into two categories. One case is shown in fig. 2.1.1, which it depicts results of the models by Coulaloglou and Tavlarides (1977), Hsia and Tavlarides(1983) and Konno et

al.(1983). The most frequent ratio of daughter and parent diameter is 0.79 which means it is likely to obtain two equal-sized daughter drops when breakage occurs.

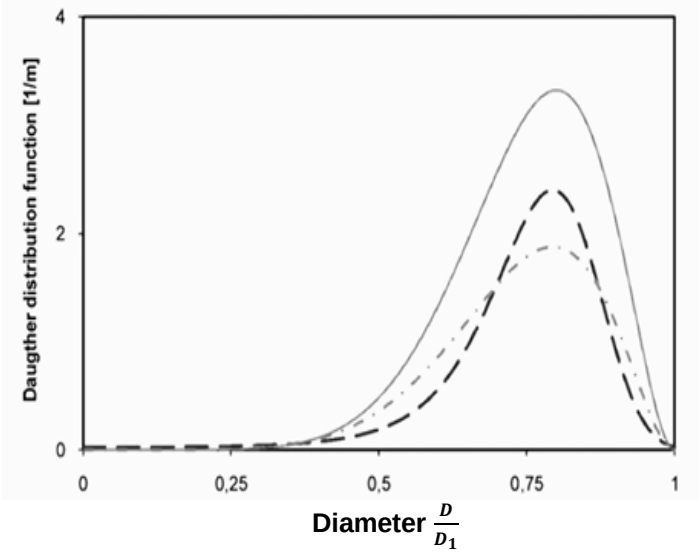

Figure 2.1.1. Comparison of β function: (----) Coulaloglou and Tavlarides (1977), (-·-·-) Hsia & Tavlarides (1983), (—) Konno et al. (1983) (Lasheras et al. 2002).

Figure 2.1.2 shows the other case of zero probability of the ratio 0.79, but it predicts very high possibilities for two kinds of daughter droplets. One is very close with parent drop on size and the other is very small daughter drop. The result is via work by Hesketh et al(1991). Due to complexity of the breakage process, mechanism has not been completely identified. For example, mass balance and drop number balance cannot be satisfied perfectly at the same time. The assumption and result are not consistent when considering the average number of daughter drops. Another point is that each kernels show great dependent on specific operation condition.

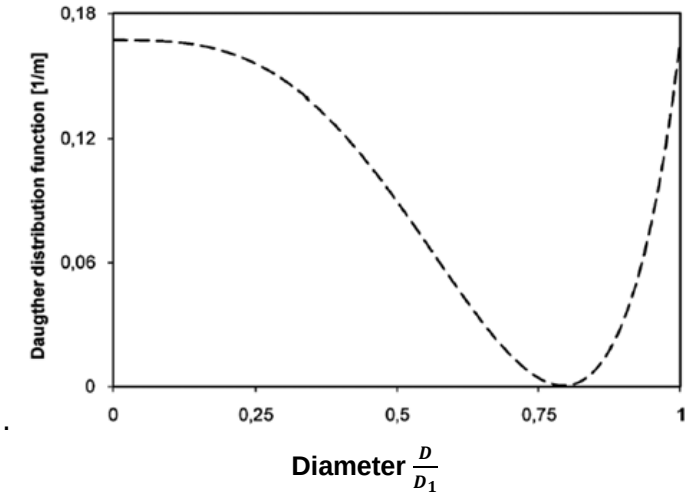

Figure 2.1.2.Variation of β function :(----) Hesketh et al (1991) (Lasheras et al. 2002).

2.1.5. Coalescence Models

Coalescence is a phenomenon in which two or more liquid droplets colloid together to form a larger droplet. In a turbulent flow field, the collision frequency is high, so the impact of coalescence is significant, but not every collision will result in coalescence. Compared with the intensive research about the breakage, investigation of coalescence phenomena is still inadequate. Models developed to explain this process mostly are based on the phenomenological model proposed by Coulaloglou and Tavlarides (1977).

According to Chatzi et al.(1989), the model describes coalescence process by dividing into two stages. Firstly, two drops approach closer and come together, but they do not coalesce immediately. A film of continuous phase still keeps them apart. Secondly, they have to be in contact with each other until the continuous phase is drained out. The time used for this process is called critical drainage time. Sometimes, the pressure fluctuate from the turbulence eddy is strong enough to pull them apart before the critical drainage time is reached.

The model assumes that collision between drops is analogous to collision between gas particles. In fact, liquid droplets do not move as fast as gas particles, the motion of droplets may not strictly follow the mechanism of random particle motion. Sometimes, coalescence will even happen immediately when two droplets collide if droplets are with enough energy and they do not bounce apart (Chatzi, 1989). Nevertheless, the model has been commonly used and satisfied results have been obtained.

Previous models only focus on the process of collision between two equal-sized drops (Marchetti and Svendsen,2012). However, Coulaloglou and Tavlarides (1977) proposed collision frequencies $\lambda(D_1, D_2)$ and coalescence efficiencies $h(D_1, D_2)$ based on the drop size to describe the coalescence rate showing high coalescence rate for one larger droplet and one small droplet, but for both two small droplets and two large droplets it shows low coalescence rate. Collision frequency and coalescence efficiencies for two drops with size D_1 and D_2 are expressed as follow respectively:

$$\lambda(D_1, D_2) = C_5 \frac{\epsilon^{1/3}}{1+\phi}(D_1 + D_2)^2({D_1}^{2/3} + {D_2}^{2/3})^{1/2} \quad (2.1.18)$$

$$h(D_1, D_2) = \exp[\frac{\epsilon\rho_c\mu_c}{\sigma^2(1+\phi)^3}\left(\frac{D_1 D_2}{D_1+D_2}\right)^4]. \quad (2.1.19)$$

Sovova(1981) indicated that the model would over predict rate of small droplets coalescence compared to larger droplets , so he proposed an energy-based coalescence efficiency expressed as follow:

$$h(D_1, D_2) = \exp[-c_7 \frac{\sigma({D_1}^2+{D_2}^2)}{\rho_d N_I^2 D_I^{4/3}({D_1}^2+{D_2}^2)}]. \quad (2.1.20)$$

This model predicates the coalescence efficiency not only for small droplets, but also for larger droplets. The model is based on the consideration that the size of droplets is at the same scale as the corresponding eddies. The coalescence will occur only if the turbulent energy of collision is larger than the surface energy of the drops. Therefore, the critical drainage time is not included in his model. In addition, the possibility that coalescence from more than two drops is relatively low, none of the models take this phenomenon into account.

In some cases, hindering the influence of the coalescence is required, so some surfactants are added into the system by changing the interfacial tension of the dispersed droplets to decrease the rate of the collision and reduce the efficiency of film drainage (Sebastian, 2011).

Whatever models have been proposed for breakage and coalescence, they all have constant parameters that need to identify by fitting experimental data. Currently, no general equation has been proposed to describe this complicated process exactly. Hence, these models are depending on the specific operated conditions.

2.1.6. Conclusion

A general population balance equation has been proposed for describing immiscible liquids dispersion in a well-mixed system. Then, this paper presented a brief review of previous breakage model, function of daughter size distribution and coalescences model. For immiscible liquid-liquid dispersion, breakage and coalescence model

developed by Coulaloglou and Tavlarides are widely used despite that some drawbacks should be corrected. Some basic mechanisms for breakage and coalescence process are identified based on the work done by other researchers. In the next stage, the PBE will be solved by using quadrature method of moments (QMOM) and empirical parameters for the models are defined by comparing measured data with simulated results.

2.1.7. References

Chatzi, E., Garrielides, A.D.& Kiparissides, C. (1989)," Generalized model for prediction of the steady-state drop size distributions in batch stirred vessels", Ind.Eng.Chem. Res. Vol 28, pp.1704-1711.

Coulaloglou, C. A., & Tavlarides, L.L.(1977),"Description of interaction processes in agitated liquid-liquid dispersions", Chem. Eng. Sci., Vol 32, pp.1289-1297.

Hesketh, R.P., Etchells, A.W.& Russell, T.W.F.(1991),"Bubble breakage in pipeline flow". Chem. Eng. Sci. Vol 46, pp.1-9.

Hsia, A.M.& Tavlarides, L. L.(1983), "Simulation analysis of drop breakage, coalescence, and micromixing in liquid–liquid stirred tanks". Chem. Eng. J. Vol 26, pp.189-199.

Kolmogoroff, A. N.(1949), "the breakup of droplets in a turbulent stream", Dokl. Akad. Nauk, Vol 66, pp.825-828.

Konno, M., Aoki, M.& Saito, S.(1983),"Scale effect on break-up process in liquid–liquid agitated tanks", J. Chem. Eng. Jpn., pp.312-319.

Luo, H.& Svendsen, F.(1996), "Theoretical model for drop and bubble break-up in turbulent dispersions". AIChE J. Vol 42,pp.1225-1233.

Lasheras, J.C.,Eastwood, C., Martinez-bazan, C.& Montanes, J. L.(2002)," A review of statistical models for the break-up of an immiscible fluid immersed into a fully developed turbulent flow", International Journal of Multiphas Flow,Vol 28, pp.247-278.

Leng,D. E. & Calabrese R.V.(2004),”Immiscible liquid-liquid systems”,(Chapter 12 in Handbook of industrial mixing, Paul, E. L., Atiemo-Obeng, V. A.& Kresta, S. M.)John Wiley and Sons, New Jersey,pp.639-742.

Marchetti, J.M. & Svendsen H.F.(2012),“Review of kernels for droplet-droplet interaction droplet-wall collision, entrainment, re-entrainment and breakage”, Chem. Eng. Comm. Vol 199, pp.551-575.

Prince, M.J.& Blanch, H.W.(1990),”Bubble coalescence and break-up in air-sparged bubble columns”, AIChE J. Vol 36,pp.1485-1499.

Shinnar, R.,(1961),’’On the behaviour of liquid dispersion in mixing vessels’’,J. Fluid Mech.10, 259-275.

Sovova, H.(1981),”Breakage and coalescence of drops in a batch stirred vessel: II. Comparison of model and experiments”, Chem. Eng. Sci., Vol 36(9),pp.1567-1573.

Tsouris, C.& Tavlarides, L.L.(1994),”Breakage and coalescence models for drops in turbulent dispersions2. AIChE J. Vol 40,pp.395-406.

Valentas, K. J., Bilous, O., & Amundson, N. R.(1966)”Analysis of breakage in dispersed phase systems”,Ind.Eng. Chem. Fundam., Vol 5,pp.271-279.

Williams, F. A.(1985),”Combustion Theory, seconded”. Benjamin/Cummings, Menlo Park, CA.

Chapter 3

3.1. Manuscript for Publication

Modelling Immiscible Liquid-Liquid Dispersion in A Stirred Tank by Population Balance Equation

Yang Yang [a], Chris D. Rielly [a,*]

[a] Department of Chemical Engineering,

Loughborough University, Loughborough,

Leicestershire, LE11 3TU, UK

* Corresponding authors:

Tel.: +44 (0) 1509 222504; fax: +44 (0) 1509 223923.

Email: C.D.Rielly@lboro.ac.uk

Abstract: A general population balance equation (PBE) is proposed for describing immiscible liquid-liquid dispersion with the solution by quadrature method of moments (QMOM). The PBE solved by QMOM has already been intensively applied to the gas-liquid dispersion and crystallisation, but not for the liquid-liquid dispersion where this study focuses on. A simulation model has been developed and tested from the aspects of the moments. The parameters for the breakage and coalescence models have been found to depend greatly on the physical properties. The predicted D_{32} is investigated with the different volume fraction of the dispersed phase and power input. It demonstrated that with higher energy dissipation rate and less fraction of the dispersed phase, the less D_{32} is achieved at steady state.

Keywords: Population balance equation; Immiscible liquids; Homogeneous; Moments; Sauter mean diameter; QMOM

3.1.1. Introduction

Many chemical processes taking place in stirred tanks involve two phases which can be solid-liquid, gas-liquid or liquid-liquid (Alopaeus et al., 1999). These multiphase systems commonly exist among the industrial application such as crystallization, polymerization or precipitation. To simulate and scale up the complex mixing processes or enhance the quality of product, it requires accurate information of evolution on droplet size distribution (DSD).

In previous works (Luo and Svendsen, 1996; Prince and Blanch, 1990; Alopaeus et al., 1999; Alopaeus et al., 2002; Marchisio et al., 2003a; Marchisio et al., 2003b; Marchisio and Fox, 2005; Gimbun et al., 2009), the population balance equation (PBE) approach has been intensively used to solve these two-phase dispersion problems. The PBE has already become the major tool for modelling mixing process. However, the precise solution for the PBE is not easy to obtain. Currently, the method of moments (MOM) and the classes methods (CM) are the two main approaches existing for providing solution of the PBE. The CM directly simulate the droplet size distribution by discretizing the internal coordinate such as droplet length or volume of population balance equation into a finite series of classes, but it normally requires massive data for each class of droplet size to work out accurate results, particularly for liquid-liquid mixing where the range of droplet size is extremely wide and complex interaction between different size of droplet sensitively affect the DSD (Marchisio et al., 2003a).

The solution given by MOM is transformation of PBE into form of moments which indicates the evolution of number density and droplet size distribution. Some scalars such as droplet length or volume may be introduced during the transformation, so it is necessary to reduce the number of scalars as few as possible to simplify the algorithm (Marchisio et al., 2003a). Among numerous methods of MOM, Quadrature method of moments (QMOM) is a simple and reliable approach. McGraw (1997) firstly introduced this method to solve the PBE for simulation of aerosol dynamics. It has also been applied for modelling of gas-liquid dispersion (Gimbun et al, 2009). Some successful results have been achieved for these applications.

In this work, the QMOM is employed to provide a solution for a PBE model of immiscible liquid-liquid dispersion in a homogeneous system where the flow is assumed to be well mixed and hence spatially homogeneous. The detail about application of the method is presented. An established model solved by QMOM is used to simulate DSD in a dispersion of n-butyl chloride in water.

3.1.2. Population Balance Equation

A general PBE for describing immiscible liquid-liquid dispersion in a stirred tank is written in a continuous form with the droplet volume as the internal coordinate as follow (Marchisio et al., 2003a) :

$$\frac{\partial}{\partial t}N(t)A(V,t) = \underbrace{\int_V^{V_{max}} \beta(V_1,V)\, m(V_1) g(V_1) N(t) A(V_1,t) dV_1}_{\text{rate of birth of droplets of volume V due to breakage}}$$

$$\underbrace{-g(V)N(t)A(V,t)}_{\text{rate of death of droplets of volume V due to breakage}}$$

$$\underbrace{+\frac{1}{2}\int_0^V \lambda(V-V_1,V_1)h(V-V_1,V_1)N(t)A(V-V_1,t)N(t)A(V_1,t)dV_1}_{\text{rate ofbirth of droplets of volume V due to coalescence}}$$

$$\underbrace{-N(t)A(V,t)\times\int_0^{V_{max}-V}\lambda(V,V_1)h(V,V_1)N(t)A(V_1,t)d\,V_1}_{\text{rate of death of droplets of volume V due to coalescence}} \quad (3.1.1)$$

Obviously, the equation above considers the influence of breakage and coalescence simultaneously, so it is also known as a general breakage-calescence equation. It is similar to the PBE describing gas-liquid dispersion, but it does not include terms of growth and nucleation, of which the influence is negligible in liquid-liquid system. The rates of the liquid flowing in and out are omitted considering a well-mixed batch system, so the mass and volume of the system is conserved and total number of droplets is only affected by the rate of breakage and coalescence. This equation is applicable to inhomogeneous system where all terms are functions of the spatial location and convection influence is inevitable but this undoubtedly increase complexity and cost of computation. Therefore, the system will be treated as well mixed.

To make the equation solvable, a further simplification is essential. By assuming the shape of all droplet is spherical, a relationship is established between droplet's

length and volume by $V \propto D^3$. Thus, Number density is introduced to replace the total number of droplets in terms of droplets diameter as internal coordinate as:

$$N(t)A(V,t) = n'(V,t); \tag{3.1.2}$$

$$n'(V,t)dV = n'(D^3,t)3D^2dD = n(D,t)dD \tag{3.1.3}$$

where $N(t)$ means the total number of droplet in the system at time t. $A(V,t)$ means the number fraction for the droplet of volume V at time t. $n'(V,t)$ means the number density for the droplet of volume V at time t. $n(D,t)$ means the number density for droplet of diameter size D at time t.

Multiplying by $3D^2$ on both sides of Eq. (3.1.1), it is rewritten in terms of droplet length (Marchisio et al.2003a; Alopaeus et al.,2006):

$$\frac{\partial}{\partial t}n(D,t) =$$

$$\int_D^{D_{max}} \beta(D,L)\, m(L)g(L)n(L,t)dL - g(D)n(D,t)$$

$$+\frac{L^2}{2}\int_o^{D_{max}} \frac{F(\sqrt[3]{D^3-L^3},L)n(L,t)n(\sqrt[3]{D^3-L^3},t)}{(D^3-L^3)^{2/3}}dL$$

$$-n(D,t)\int_0^{\sqrt[3]{D_{max}^3-L^3}} \lambda(D,L)h(D,L)n(L,t)d\,L \tag{3.1.4}$$

where F represents coalescence rate resulted from the collision frequency $\lambda(\sqrt[3]{D^3-L^3},L)$ and collision efficiency $h\left(\sqrt[3]{D^3-L^3},L\right)$.

Generally, rigorous modelling of such a complex dispersion is a computationally intensive task by using discrete population balance (DPB). Large amount of statistics of droplet size distribution is required to provide accurate predicted results. The introduction of the moment transformation makes it possible to solve the PBE without enormous data and accuracy of result is still acceptable. Another obvious advantage is improvement of the computational efficiency by converting PBE to the equation in terms of the moments. Meanwhile, sufficient information about the droplet size distribution can be obtained to predict the evolution of the DSD (Falola et al., 2013).

Transforming Eq. (3.1.4) into moments using:

$$\mu_k = \int_0^\infty n(D,t)D^k dD \tag{3.1.5}$$

where k indicates number of moment, the PBE is written as:

$$\frac{d}{dt}\mu_k = \int_0^\infty D^k \int_D^{D_{max}} \beta(D,L)\, m(L) g(L) n(L,t) dL dD - \int_0^\infty D^k g(D) n(D,t) dD + \frac{1}{2}\int_0^\infty D^k \int_o^{D_{max}} \lambda\left(\sqrt[3]{D^3 - L^3}, L\right) h\left(\sqrt[3]{D^3 - L^3}, L\right) n(L,t) n\left(\sqrt[3]{D^3 - L^3}, t\right) dL dD - \int_0^\infty D^k\, n(D,t) \int_0^{\sqrt[3]{D_{max}^3 - L^3}} \lambda(D,L) h(D,L) n(L,t) d\, L dD \tag{3.1.6}$$

It is now possible to numerically integrate Eq. (3.1.6) by using quadrature approximation, generally which is written as (McGraw,1997):

$$\mu_k = \int_0^\infty n(D,t)D^k dD \approx \sum_{i=1}^N w_i D_i^k \tag{3.1.7}$$

where weights w_i are calculated from the lower-order moments and D_i are corresponding abscissas. The first step of transformation is the construction of a matrix P with components $P_{i,j}$ starting from the moments (Marchisio et al. 2003a)..

The 1st column of P are

$$P_{i,1} = \delta_{i1}, i = 1,2,3,\ldots,2N+1 \tag{3.1.8}$$

Where δ_{i1} is the Kronecker delta.

The components in the 2nd column of P are:

$$P_{i,2} = (-1)^{i-1} m_{i-1}, i = 1,2,3,2N+1 \tag{3.1.9}$$

The rest column of P are obtained from

$$P_{i,j} = P_{1,j-1}P_{i+1,j-2} - P_{i,j-2}P_{i+1,j-1}, j = 3,4,\ldots,2N+1 \; and \; i = 1,2,3,2N+2-j \tag{3.1.10}$$

For example,$2N = 2$, then P becomes:

$$P = \begin{bmatrix} 1 & 1 & \mu_1 & \mu_2 - u_1^2 & \mu_3\mu_1 - \mu_2^2 \\ 0 & -\mu_1 & -\mu_2 & -\mu_3 + \mu_2\mu_1 & 0 \\ 0 & \mu_2 & \mu_3 & 0 & 0 \\ 0 & -\mu_3 & 0 & 0 & 0 \\ 0 & 0 & 0 & 0 & 0 \end{bmatrix} \quad (3.1.11)$$

The coefficient of the continued fraction (α_i) are produced by defining 1st element to 0($\alpha_1 = 0$) and computing the others according to:

$$\alpha_i = \frac{P_{1,i+1}}{P_{1,i}P_{1,i-1}}, i = 2, \dots 2N \quad (3.1.12)$$

A symmetric tridiagonal matrix is obtained from sums and products of α_i,

$$a_i = \alpha_{2i} + \alpha_{2i-1}, i = 1, \dots, 2N - 1 \quad (3.1.13)$$

and

$$b_i = \alpha_{2i} + \alpha_{2i-1}, i = 1, \dots, 2N - 1 \quad (3.1.14)$$

Where a_i and b_i are the diagonal and the subdiagonal of the Jacobi matrix. When the tridiagonal matrix is determined, the weights and abscissas are determined by finding its eigenvalues and eigenvectors. The eigenvalues are found form:

$$w_j = \mu_0 v_{j1}^2 \quad (3.1.15)$$

Where v_{j1} is the first component of the jth eigenvector. All these values are numerically calculated using MATLAB.

Recently, a moment method was proposed and tested by Alopaeus et al. (2006), which calculated the integrals with fixed quadrature points and corresponding moment-conserving weights. The fixed quadrature points are also defined by some pre-determined conditions, of which the simplest choice is to use zeros of orthogonal polynomials (Alopaeus et al., 2006). It overcomes the problem that only an even number can be set for the algorithm. Nevertheless, the fixed quadrature method of moments (F-QMOM) is very similar to QMOM, and it does not show distinctive improvement on the accuracy. Thus, QMOM rather than F-QMOM will be applied in the current work. Marchisio and Fox (2005) also proposed a method called direct quadrature method of moments (DQMOM) which solves quadrature points and weights directly. It is said to show better performance than QMOM, especially when

multi-compartments are investigated coupled with computational fluid dynamics (CFD). Considering that the current work just treats the system as a single compartment then this method is also not necessary as well.

Applying the QMOM transformation, Eq. (3.1.6) is converted into a discrete form:

$$\frac{\mathrm{d}}{\mathrm{dt}}\mu_{\mathrm{k}} = \sum_{\mathrm{i}=1}^{\mathrm{n}} \mathrm{m}(\mathrm{D_i})\mathrm{g}(\mathrm{D_i})\mathrm{F_i^k}\,\mathrm{w_i} - \sum_{\mathrm{i}=1}^{\mathrm{n}} \mathrm{D_i^k g}(\mathrm{D_i})\mathrm{w_i} + \frac{1}{2}\sum_{\mathrm{i}=1}^{\mathrm{n}} \mathrm{w_i} \sum_{\mathrm{j}=1}^{\mathrm{n}} \mathrm{w_j}\left(\mathrm{D_i^3} + \mathrm{D_j^3}\right)^{\frac{\mathrm{k}}{3}} \lambda\left(\mathrm{D_i}, \mathrm{D_j}\right)\, \mathrm{h}\left(\mathrm{D_i}, \mathrm{D_j}\right) - \sum_{\mathrm{i}=1}^{\mathrm{n}} \mathrm{D_i^k w_i} \sum_{\mathrm{j}=1}^{\mathrm{n}} \mathrm{w_j}\lambda\,(\mathrm{D_i}, \mathrm{D_j})\mathrm{h}\left(\mathrm{D_i}, \mathrm{D_j}\right) \qquad (3.1.16)$$

where $\mathrm{F_i^k} = \int_0^\infty \beta(\mathrm{D}, \mathrm{D_i})\mathrm{D^k dD}$.

Terms involving the droplet number density no longer exist in the equation anymore. By providing appropriate breakage and coalescence expressions, the equation is solvable. The equation is also applicable to gas-liquid dispersion, but current work only focuses on the liquid-liquid dispersion. The models developed by Coulaloglou and Tavlarides(1977) for describing breakage and coalescence were employed due to their successful prediction on the DSD reported in the previous work. More details about other models can be found in the review done by Lasheras et al. (2002).

3.1.3. Rate functions

In the past few decades, the most widely used model is a phenomenological model proposed by Coulaloglou and Tavlarides(1977). It assumes that both the dispersed phase and continuous phase are moving at the same velocity in a locally isotropic turbulent system, so there is no relative velocity between dispersed phase and continuous phase (Azizi, et al. 2011). In addition, chemical reaction is not happening in the system, so the system is treated isothermally. The behaviours of the breakage and coalescence are mainly caused by the turbulence eddies in the system. An obvious advantage of the model is its ability to take onto account the influence of the physical and hydrodynamical properties of the system by formulating semi-empirical models containing a few numbers of parameters. These parameters can be modified to apply the model into the specific condition where different levels of power input and different levels of dispersed phase volume fraction are

investigated. Currently, large amount of models are built according to the phenomenological model (Azizi and Al Taweel, 2011).

3.1.3.1. Breakage Models

Generally, the breakage model is described as a result from a combination of breakage frequency and breakage efficiency. The breakage frequency means how many droplets are likely to break in a unit time. It is determined by the force on the surface of the droplet generated from the collision between droplets and turbulence eddies. The breakage efficiency means the chance a droplet will break successfully in the end. Sometimes, a droplet may be squeezed by the turbulence eddy in one point, but it moves to somewhere far away from the impeller region and the force on the surface becomes smaller before it is broken. Therefore, the breakage is described as a probability event. A specific breakage frequency of droplets of drop size D_i in a turbulent field characterised by dissipation rate ε and the dispersed phase volume fraction ϕ is written as follow: (Azizi and Al Taweel, 2011; Alopaeus et al.2002; Coulaloglou and Tavlarides, 1977):

$$g(D_i) = C_1 \frac{\varepsilon^{1/3}}{D_i^{2/3}(1+\phi)} \times \exp[-C_2 \frac{\sigma(1+\phi)^2}{\rho_d \varepsilon^{2/3} D_i^{5/3}}] \quad (3.1.17)$$

The drawback of the rate function is the absence of taking the viscosity of dispersed phase into account, but it has been tested as a valid assumption by Andersson and Andersson (2006). About this point, many different opinions have been proposed as it is still an unsettled factor for liquid-liquid dispersion where viscosity of the dispersed phase might show influence on the number of daughter drops. Nevertheless, the model was employed to predict the DSD in this work as it has been demonstrated as a successful model so far.

3.1.3.2. Daughter Droplets Distribution

An expression for daughter size distribution, given by Coulaloglou and Tavlarides(1977), presents probability for specific size of daughter droplet resulted from a bigger parent droplet, but it is purely statistical function based on normal distribution developed by Valentas (1966):

$$\beta(D, D_i) = \frac{4.6}{D_i^3} \exp(-4.5 \frac{(2D^3 - D_i^3)^2}{(D_i^3)^2}) \quad (3.1.18)$$

where $\beta(\mathrm{D},\mathrm{D_i})$ means frequency of daughter drops of diameter D resulting from breakage of parent drops of diameter D_i.

One obvious problem for Eq.(3.1.18) is that it only shows zero probability for the daughter droplet with the same size as its parent droplet, but not for infinite small droplets. It means that there is a possibility for the daughter droplet of diameter 0 to be formed. It is wrong obviously. A more sophisticated and accurate beta function was developed by Hisa and Tavlarides (1980) shown in Fig.3.1-2 (H&T). The main advantage for this distribution is that zero probability is calculated for both infinitely small daughter droplet and daughter droplet with same size as the parent droplet. The function is written as (Hisa and Tavlarides,1980):

$$\beta(\mathrm{D},\mathrm{D_i}) = 90\frac{\mathrm{D}^2}{\mathrm{D_i^3}}\left(\frac{\mathrm{D}^3}{\mathrm{D_i^3}}\right)^2(1-\frac{\mathrm{D}^3}{\mathrm{D_i^3}})^2 \tag{3.1.19}$$

The L, E&G in Fig.3.1-2 means the function developed by Lee et al. (1987). It provides very similar function with the model by Hisa and Tavlarides (1980), but the curves are not similar. The equation is shown as:

$$\beta(\mathrm{D},\mathrm{D_i}) = \frac{\Gamma(\mathrm{a+b})}{\Gamma(\mathrm{a})\Gamma(\mathrm{b})D_i}\left(\frac{\mathrm{D}}{D_i}\right)^{\mathrm{a-1}}(1-\frac{\mathrm{D}}{D_i})^{\mathrm{b-1}}, \tag{3.1.20}$$

where a and b are empirically derived constants. For binary breakage, Lee et al. think the value for both a and b was 2. The curve shown in Fig.3.1-1 is result for this case.

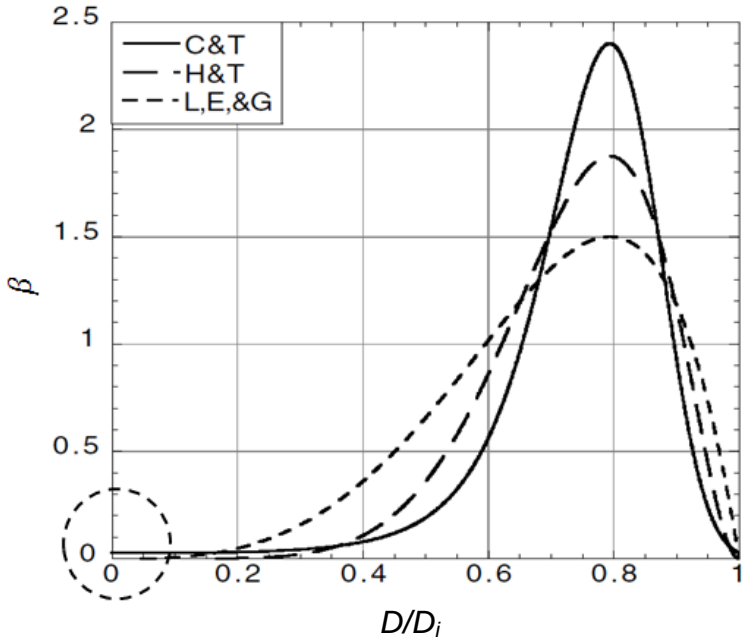

Figure 3.1-1. Daughter droplet size distribution for different beta functions (Lasheras et al., 2002)

All these functions present the maximum value of β is achieved at the diameter ratio of 0.8, which means that two equal size daughter droplets are likely to formed. Therefore, it is reasonable to use a symmetric fragmentation function developed by Marchisio et al. (2003). It defines two equal size daughter droplets will be formed due to the breakage and it has been related to the diameter of the parent droplet diameter written as:

$$\begin{cases} 2 \text{ if } \mathrm{D} = \frac{\mathrm{D_i}}{2^{\frac{1}{3}}} \\ 0 \text{ otherwise} \end{cases}. \tag{3.1.21}$$

In the simulation, all three cases have been tested and the symmetric fragmentation function presented more reasonable results than others, so it has been chosen to present simulation results.

3.1.3.3. Coalescence Model

The rate function for describing the phenomenon of coalescence includes two terms. One is function of collision frequency and the other is function of collision efficiency. The function was first developed by Coulaloglou and Tavlarides (1977), but Hisa and Tavlarides (1983) pointed out an obvious mistake by changing $\left(\mathrm{D_i}^2 +\right.$

$D_j^2)$ into $(D_i + D_j)^2$ for collision frequency. The modification has been supported by most researchers (Maab et al. 2010, Azizi et al., 2011)

The collision frequency is written as:

$$\lambda(D_i, D_j) = C_3 \frac{\varepsilon^{1/3}}{1+\phi}(D_i + D_j)^2 (D_i^{2/3} + D_j^{2/3})^{1/2} \quad (3.1.22)$$

The collision efficiency is written as:

$$h(D_i, D_j) = \exp(-C_4 \frac{\mu_c \rho_c \varepsilon}{\sigma^2 (1+\phi)^3} (\frac{D_i D_j}{D_i + D_j})^4) \quad (3.1.23)$$

Combining these two equations, the rate of coalescence is shown as:

$$F(D_i, D_j) = C_3 \frac{\varepsilon^{1/3}}{1+\phi}(D_i + D_j)^2 (D_i^{2/3} + D_j^{2/3})^{1/2} \exp(-C_4 \frac{\mu_c \rho_c \varepsilon}{\sigma^2 (1+\phi)^3} (\frac{D_i D_j}{D_i + D_j})^4) \quad (3.1.24)$$

where σ is interfacial tension for the liquid-liquid system.

The mechanisms for droplet coalescence are mainly based on buoyancy (gas-liquid dispersion), collision due to laminar shear forces and turbulent interaction (Prince and Blance, 1990; Marchetti and Svendsen, 2012). As the target system is assumed to be a highly turbulent liquid-liquid dispersion, only the turbulent interaction is considered. The coalescence is mainly affected by the forces caused by the turbulent pressure which lead to draining of the film between two droplets until it ruptures. Sometimes, two droplets may be separated by the turbulent pressure fluctuations because kinetic energy of the eddy is not strong enough to maintain them together till the coalescence is completed. The function above generally gives sufficient description of this phenomenon.

Compared with extensive work for the breakage, the investigation of calescence is limited and not many models have been presented because the phenomenon has not been understood completely.

3.1.4. Results and Discussion

The aim of the investigation was to test the model with a parameter fitting procedure in n-butyl chloride/water system involving breakage and coalescence occurring simultaneously. The simulated results were compared with experimental data in terms of the moments and the Sauter mean diameter. Then, the empirical constants for the models were defined through fitting measured data with simulated results. Applying the models with estimated parameters, the dynamic Sauter mean diameter against time was investigated under different power consumptions and fractions of the dispersed phase.

3.1.4.1. Experimental Data

The experimental data was taken from the work done by Maab et al. (2012) due to its detailed experimental information. A model system was set up for simulating a dispersion of n-butyl chloride in water with the dispersed phase fraction of 25% at atmospheric pressure and 20 °C. The purity for n-butyl chloride was beyond 99.98% and water was deionized. Impurities should be ensured to be excluded, because it may have impact on both rates of breakage and coalescence. Under these conditions, the density of water is 997 kg/m^3 and viscosity is 1x10^{-3} Pa·s. The density of n-butyl chloride is 886kg/m^3 and the viscosity is 0.427x10^{-3} Pa·s. The interfacial tension for n-butyl chloride /water is a key factor affecting greatly on the coalescence phenomenon. It can be affected by the surfactant of Poly Vinyl Alcohol (PVA), which is introduced into the tank to reduce the impact of the coalescence. The concentration of PVA was 0.1mg/g (mass of PVA over mass of n-butyl chloride) and corresponding interfacial tension of n-butyl chloride /water was 9.8 x10^{-3} N/m shown in Fig. 3.1-2.

As the total amount of PVA is relative small compared with the volume of the continuous phase, the properties of the water are still regarded as properties of the continuous phase and not affected by the PVA (Maab et al. 2012).

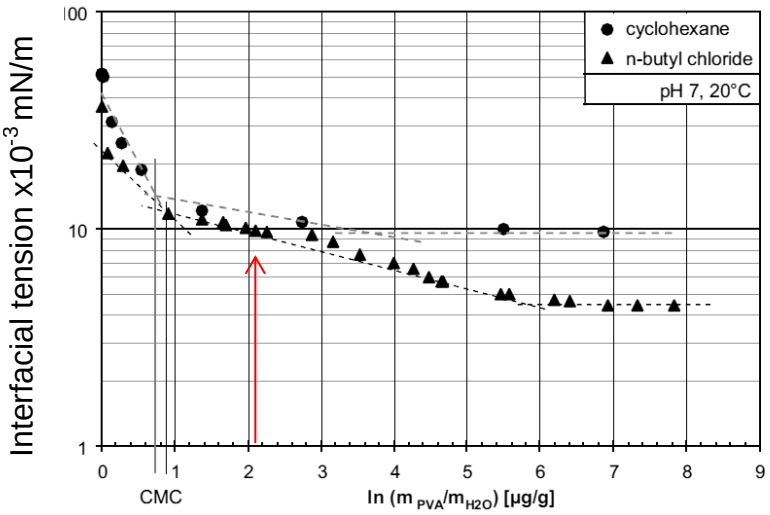

Figure 3.1-2. The interfacial tension of n-butyl chloride/water against the various concentrations of PVA (Maab et al. 2012).

The dimensions of the vessel used for measuring droplet diameter distribution are shown in Table 3.1-1 and Fig.3.1-3.

Table 3.1-1. The detail of dimensions of the tank (Maab et al. 2012).

T	H/T	l_B/H	d/T	h_{st}/d	h/d	S_B/T
155mm	1.4	1.0	0.55	0.06	1.8	0.08

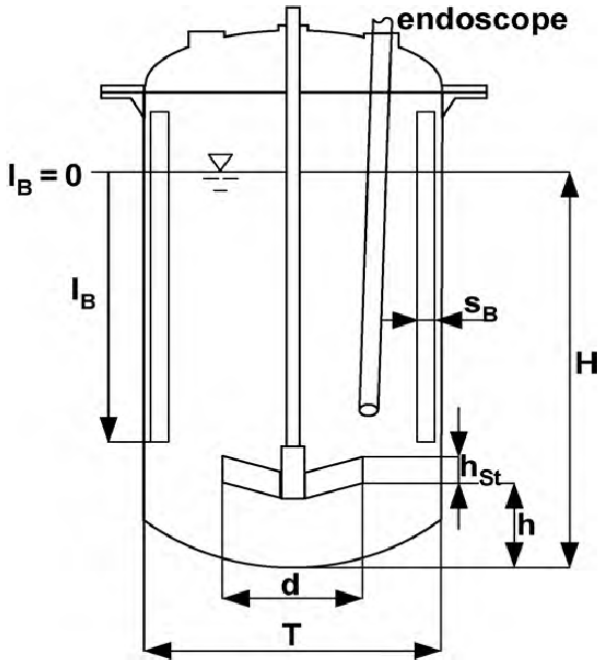

Figure 3.1-3. Experimental set-up and dimensions of the tank (Maab et al., 2012)

The speed of a blade impeller N_{speed} is 410 rpm. As power consumption is a major factor investigated in the work, the energy dissipation rate is required and can be calculated by following equation:

$$\varepsilon = \frac{P}{V_{tank}\rho_{ave}} \tag{3.1.25}$$

where V is volume of the vessel and it is calculated as 4.026x10^{-3} m^3 at H/T of 1.4 and the input power P is calculated according to power number based on:

$$Ne = \frac{P}{\rho_{ave} N_{speed}^3 d^5} \tag{3.1.26}$$

The density is average value of the water and n-butyl chloride and it is 970kg/m^3 for dispersed phase fraction of 0.25. The power number Ne measured under this case is 0.86, so energy dissipation rate is calculated as 0.307m^2/s^3. A set data of cumulative number distributions was measured at some specific time points (1, 3, 5 10 and 40 minutes).

The normal distribution is not used as it shows non-zero number density for the droplet of diameter 0 and it also shows non-zero number density for the droplet of negative diameter in Fig.3.1-4. However, the log-normal distribution function shows satisfactory agreement for five sets of measured data.

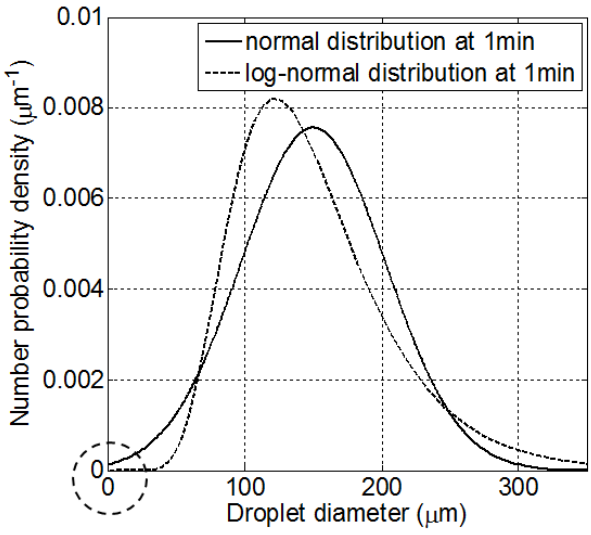

Figure 3.1-4. Comparison of normal distribution and log-normal distribution.

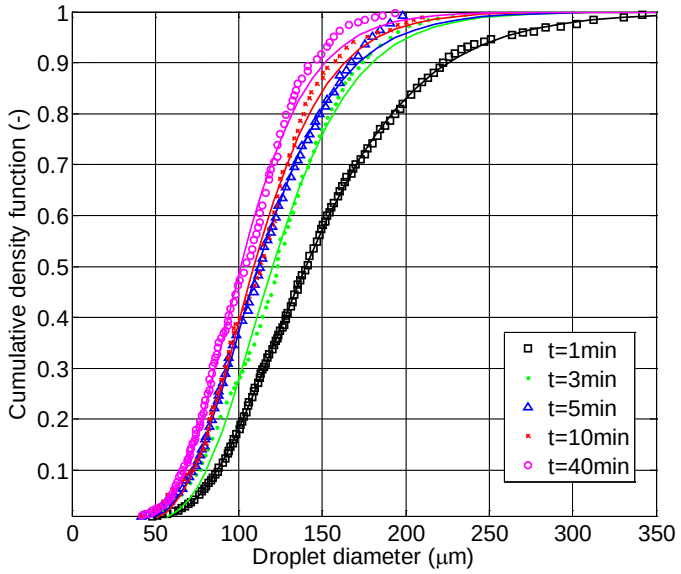

Figure 3.1-5. Cumulative densities against droplet diameters at different time points

Fig. 3.1- 5 shows the evolution of cumulative droplets size distribution at several time points. The log-normal distribution was employed to fit with the measured data. The function is written as:

$$f(D,\mu,\sigma) = \frac{1}{D\sigma\sqrt{2\pi}}\exp\left(-\frac{(\ln D-\mu)^2}{2\sigma^2}\right) \tag{3.1.27}$$

where μ is related to the geometric mean D_{geo} through the equation $D_{geo} = e^{\mu}$ and σ is standard deviation of the variable D.The integral of $f(D,\mu,\sigma)$ refers to the cumulative log-normal distribution, which is possibly shown as an error function, but it has no analytical form. However, the parameters of σ and μ are possible to obtain by parameters fitting procedure and make it possible to generate the 1st moment ~5th moment through the equations shown below:

$$\begin{cases} \mu_1 = \exp(\mu + \frac{1}{2}\sigma^2) \\ \mu_2 = \exp(2\mu + \frac{4}{2}\sigma^2) \\ \mu_3 = \exp(3\mu + \frac{9}{2}\sigma^2) \\ \mu_4 = \exp(4\mu + \frac{16}{2}\sigma^2) \\ \mu_5 = \exp(5\mu + \frac{25}{2}\sigma^2) \end{cases} \tag{3.1.28}$$

The 0th moment means the total number density of droplets, so μ_0 should be constant one. μ_1 means the total diameter of droplets per unit volume; μ_2 means the

total area of droplets per unit volume and μ_3 means the volume fraction of dispersed phase. μ_4 and μ_5 do not have realistic physical meaning (Marchisio et al. 2003a).

The moments at time 0 were obtained by linear extrapolation from the moments at later times. Then, the measured moments at each time points were used to obtain estimates of the best fit parameter for breakage and coalescence functions

3.1.4.2. Simulation results

The simulated results were calculated through the quadrature approximation:

$$\mu_k = \int_0^\infty n(D,t)D^k dD \approx \sum_{i=1}^{N} w_i D_i^k \qquad (3.1.29)$$

where weights w_i and abscissas D_i are determined by the product-difference(PD) algorithm. There is no physical meaning for both abscissas and weights for the quadrature approximation, because they are just some intermediate numbers derived from the PD algorithm. However, they can be seen as an approximation for the DSD. The abscissa corresponds to the droplet class size and the weight is related to relative frequency of droplet in each classes. Fig. 3.1-6 shows the initial abscissas and corresponding weights converted from the initial 6 moments at time 0 by extrapolation from the variation of the moments at later time. Although it is not rigours, it still reflects the droplets size distribution to some extent. During the process of calculation, the abscissas moves along with the droplet size axis, so it reflects the dynamic evolution of droplets size distribution (Marchisio et al 2003a).

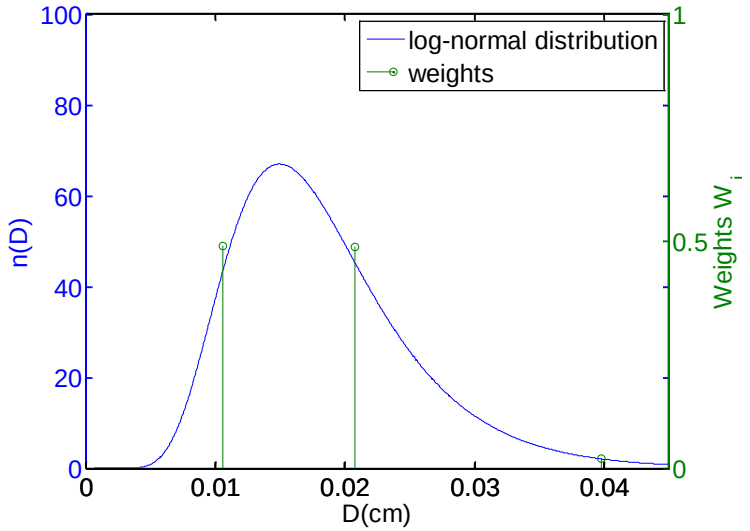

Figure 3.1-6. Initial abscissas and weights transformed from log-normal distribution.

The QMOM does not predict DSD directly, which is unlike discrete methods, but it is possible to reconstructed from the moments. In this work, only moments were tracked for analysis. The first six moments (0th ~5th moment) were obtained at the number of quadrature point N=3. As a higher number of quadrature point (N) does not necessarily increase the accuracy of simulation and there is no obvious gain in accuracy of QMOM prediction (Marchisio et al 2003a), so the quadrature point was set as 3 for PD algorithm. The ratio of the 3rd moment and the 2nd moment generates dynamical evolution of the Sauter mean diameter (D_{32}) and it was compared with measured data.

Table 3.1-2 shows detail about the initial weights and abscissas. The sum of all weights equals exactly to one which equals exactly to the value of 0th moment. It demonstrated the correct conversion by PD algorithm.

Table 3.1-2. The detail about initial abscissas and weights.

w_1	0.4896	D_1	0.0106(cm)
w_2	0.4885	D_2	0.0208(cm)
w_3	0.0219	D_3	0.0397(cm)

Fig.3.1-7 shows the evolution of all six moments against time within 40 minutes. The simulated results were compared with the measured data at time 1, 3, 5, 10 and 40 minutes. The detail of measured data was presented in Table 3.1-3. Except for the 1st moment, the rest moments are regarded as steady state at time 40 minutes, because they showed almost the same shape of the lines by setting enough long time (longer than 120 minutes) for simulation. At dynamic equilibrium state, the lines are nearly horizontal indicating the system is almost steady, where the rate of breakage equals to the rate of coalescence. Specifically, at 40 minutes, the difference of the rate of breakage and coalescence was -7.72x10^{-14}, an extremely small number, which indicates the difference between rate of breakage and rate of coalescence is negligible.

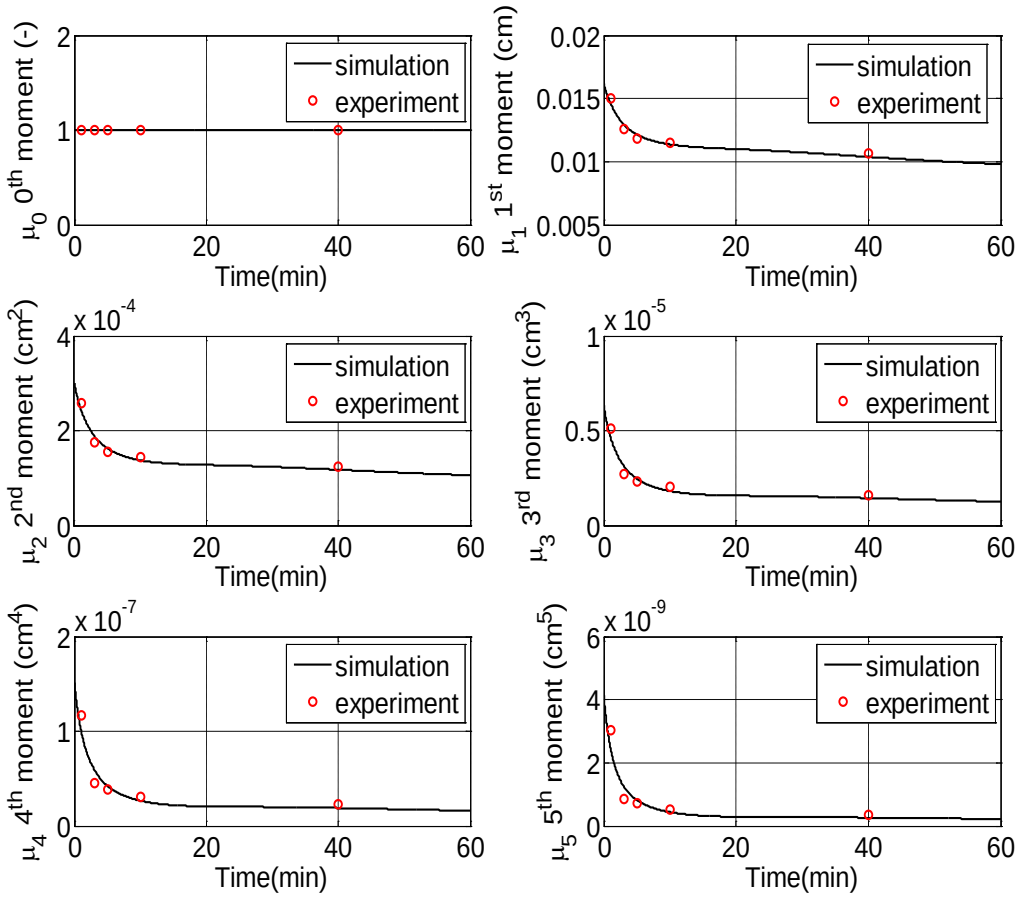

Figure 3.1-7. Evolution of the first six moments compared with the measured data.

In order to examine the validation of the established models, an overall error was defined as:

$$E=\sum_{i=1}^{n}(\gamma_i)^{-2}\sum_{i=1}^{n}[\mu_i-\mu_i^*]^2 \qquad (3.1.30)$$

where μ_i^* represents the real moment derived from the experimental data and $\gamma_i=\mu_i(\text{initial})^{-1}$. As the magnitude of the each moment varies significantly, the contribution to the overall error is not on the same scale, so γ_i is introduced to balance influence of errors resulted from each moment. It is important to note that all the simulated moments are normalised by the total number of droplets in the system by

$$\mu_i=\frac{\mu_i'}{u_0} \qquad (3.1.31)$$

so the simulation results are based on the number density. Details about moments calculated from experimental data are shown in Table 3.1-3.

Table 3.1-3. The first six moments calculated from the experimental data at time 1, 3, 5, 10, 40 minutes and values extrapolated by linear extrapolation

	μ_0	$\mu_1(cm)$	$\mu_2(10^{-4}(cm^2))$	$\mu_3(10^{-6}cm^3)$	$\mu_4(10^{-8}cm^4)$	$\mu_5(10^{-10}cm^5)$
Initial	1	0.0162	3.0018	6.3294	15.16	41.234
1 min	1	0.015	2.587	5.1189	11.629	30.331
3 min	1	0.0126	1.7575	2.6979	4.567	8.5251
5 min	1	0.0118	1.5619	2.3122	3.8324	7.112
10min	1	0.0115	1.4499	2.0242	3.1185	5.3024
40min	1	0.0106	1.2471	1.6146	2.3073	3.6387

The contribution of the errors for each moment is shown in table 3.1-4. The overall error after optimisation is 7.07% which is acceptable considering that it is a sum of error resulted from the each moment. It is interesting to note that the error from the lower moments is smaller than the error from the higher moments. This is in agreement with the work done by Randolph and Larson (1971). They believed that the higher moments unduly weight the distribution towards the larger size droplets**.**

Table 3.1-4. The detail about the errors for the first 6 moments.

	μ_0	μ_1	μ_2	μ_3	μ_4	μ_5
$[\mu_i - \mu_i{}^*]^2$	0	4.71×10^{-7}	5.54×10^{-10}	5.11×10^{-13}	4.78×10^{-16}	4.98×10^{-19}
$(\gamma_i)^{-2}[\mu_i - \mu_i{}^*]^2$	0	0.18%	0.61%	1.28%	2.08%	2.93%

Fitting simulated results to the experimental data, the four parameters ($C_1, C_2, C_3\ and\ C_4$) of the model by Coulaloglou and Tavlarides (1977) were defined . Due to its success, it seems be regarded as a standard model for modelling liquid-liquid mixing. Previous work has presented some values for these parameters, but they are presented just as reference (Table 3.1-5) since the liquid-liquid system and geometries of the tank of the current work are very different from which used in their work. The values used in the work are several orders of magnitude larger than the previous ones mainly due to the simplifying assumption of uniform system. In the current work, C_1, C_2, C_3, C_4 are defined as $3.3681 \times 10^{-4}, 0.0582, 0.2607, 1.8994 \times 10^{10}(m^{-2})$ respectively. These valuse are obtained by minimise the error E ($E=\sum_{i=1}^{n}(\gamma_i)^{-2}\sum_{i=1}^{n}[\mu_i - \mu_i{}^*]^2$) to 7.07% and they are kept unchanged throughout the

whole study for predication as they were believed to be independent of the operation conditions. The optimisation tool *fmincon* in MATLAB(R2012a) was employed provide the results.

Table 3.1-5. The specific values for empirical parameters.

Empirical Constants	C_1	C_2	C_3	$C_4(m^{-2})$
Coulaloglou and Tavlarides(1977)	$4.871x10^{-3}$	0.0552	$2.17x10^{-4}$	$2.28x10^{+13}$
Hisa and Tavlarides (1980)	0.01031	0.06354	$4.5x10^{-4}$	$1.891x10^{+13}$
Azizi et al. (2011)	0.86	4.1	0.04	$1.0x10^{+10}$
Current work	$3.3681x10^{-4}$	0.0582	0.2607	$1.8994x10^{+10}$

Overall, the simulation results for 0th~5th moments are satisfactory and the estimated four empirical parameters are used to predicate the D_{32} under different energy dissipation rates and fractions of dispersed phase.

3.1.4.3. Prediction of D_{32}

The predicted Sauter mean diameter (D_{32}) was compared with the measured data calculated from the model system where the impeller speed was 410 rpm and the fraction of the dispersed phase was 25%.

In Fig. 3.1-8, apart from the measured data at points of time 3 minutes and 10 minutes are slightly away from the simulated line. The rest presents acceptable agreement and the relative error is within 5%. The Sauter mean diameter at time 40 minutes was 4.9% away from the experimental value. Nevertheless, the simulated line predicates a correct trend for achieving steady state for D_{32} at fraction of dispersed phase of 25%. Despite the simulated results present satisfactory agreement on the moments, it does not ensure the accurate prediction of D_{32}. Due to the complex of the flow regions in the tank, the average energy dissipation rate is several orders of magnitude higher near the impeller than far from it. The average energy dissipation rate cannot reflect the real power consumption when D_{32} was reduced sharply. If the system was divided into several sub-regions modelling with local energy dissipation rate, a better result would be obtained.

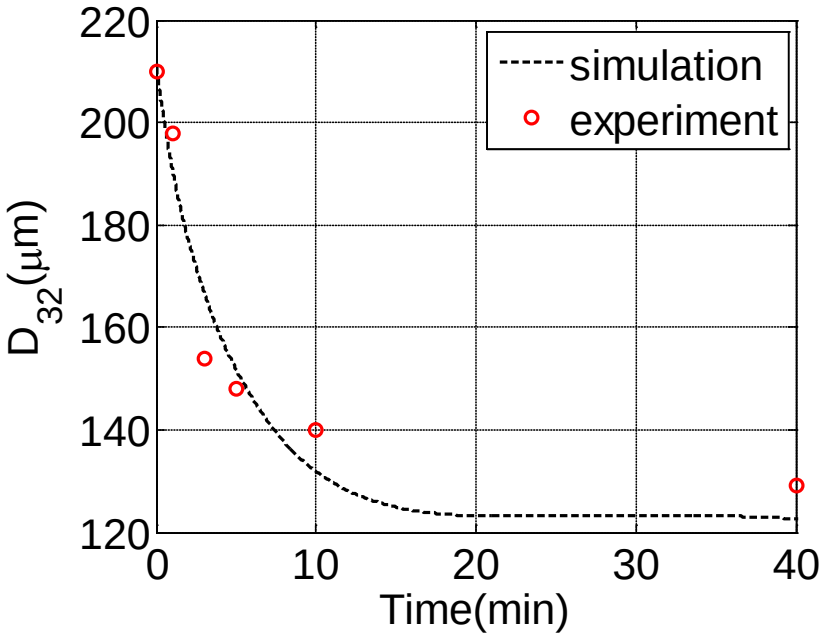

Figure 3.1-8. Evolution of the Sauter mean diameter at fraction of the dispersed phase 25%, within 40 minutes compared with measured data.

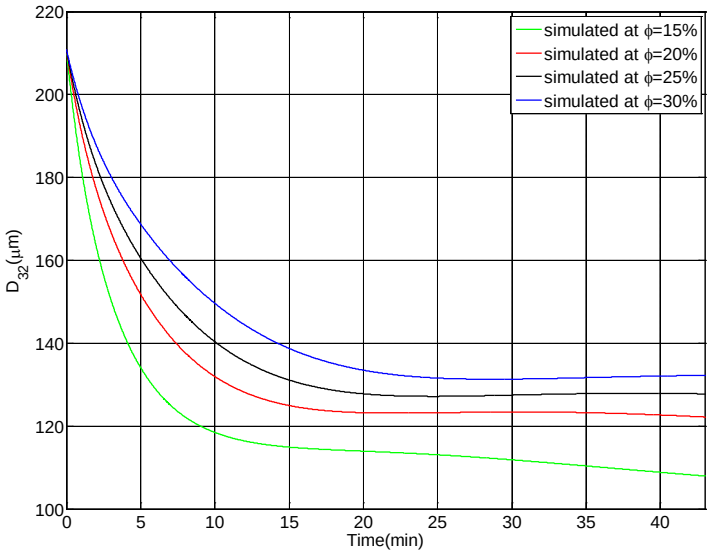

Figure 3.1-9. Evolution of the Sauter mean diameter at fraction of dispersed phase 15% 20% 25% and 30% within 40 minutes.

In Fig.3.1-9, the final Sauter mean diameters at time 40 minutes are 108.8μm, 122.6μm, 127.8μm and 132.1μm for fraction 15% 20% 25% and 30% respectively. Keeping the impeller speed unchanged, the influence of the fraction of the dispersed phase was investigated with the optimised parameters. For the higher fraction of the dispersed phase, the larger D_{32} was achieved in the end. It means even average

energy dissipation rate is the same for each case. The final equilibrium state is varied under different volume fraction of the dispersed phase.

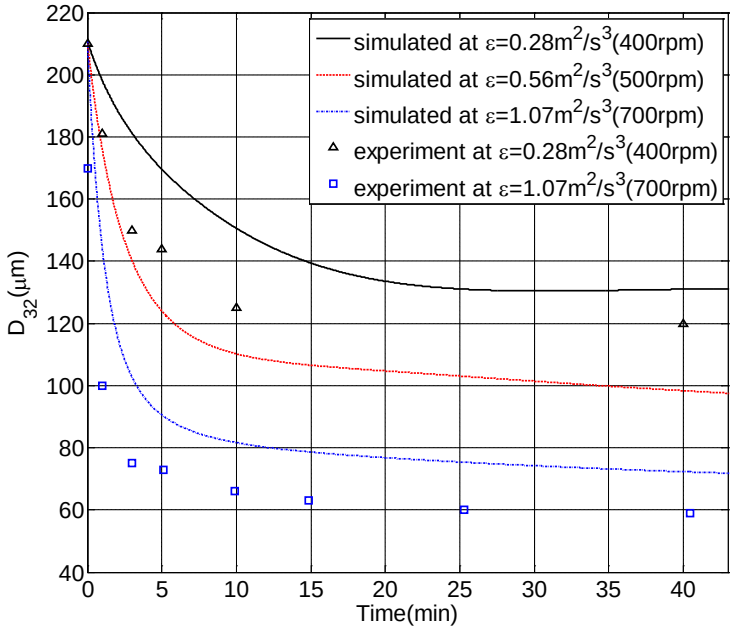

Figure 3.1-10. Evolution of the Sauter mean diameter at impeller speed of 400,500,700 rpm within 40 minutes.

The different energy dissipation rates were also investigated by keeping other operation conditions unchanged. The experiment was conducted under the fraction of dispersed phase of 45% with impeller speed ranging from 400rpm to 700rpm.In Fig.3.1-10, the predicted D_{32} are all larger than the measured D_{32}. At time 40 minutes, the predicted D_{32} (131.01 μm) is larger than the experimental D_{32}(121.0 μm) by 8.26% for ε with 0.28 $m^2 \cdot s^{-3}$. In the case that ε equals 1.07 $m^2 \cdot s^{-3}$, the predicted D_{32} for steady state is 72.32μm larger than experimental D_{32}(60 μm) by 12.32 μm.

These errors were mainly caused by concentration of PVA was changed from 0.1mg/g to 1mg/g, which resulted in variation of the interfacial tension of the dispersed phase from 9.8 mN/m to 8 mN/m. Changing concentration of PVA, the impact is greater on the rate of coalescence than the rate of breakage in the simulation. It means the rate of coalescence is increased much more. The larger droplets are formed while the rate of breakage is still unchanged or increased slightly.

Increasing the speed of the impeller from 400rpm (0.28 $m^2 \cdot s^{-3}$) to 500rpm (0.56 $m^2 \cdot s^{-3}$) and 700rpm(1.07 $m^2 \cdot s^{-3}$), the predicted D_{32} at time 40 minutes were reduced by increasing the power input. The detail about the energy dissipation rate and relevant final D_{32} is shown in Table 3.1-6.

Table 3.1-6. Energy dissipation rate against D_{32} at equilibrium state (um)

Energy dissipation rate($m^2 \cdot s^{-3}$)	D_{32} at equilibrium state(μm)
0.28	131.01
0.56	98.39
1.07	72.32

It can also be observed in Fig.3.1-11 that the time for reaching equilibrium state was also delayed for lower energy input. N*t represents the time that was normalised by multiplying the corresponding impeller speed and the θ represents the normalised Sauter mean diameter by:$\theta = \frac{D_{32}-D_{32}(initial)}{D_{32}(infinity)-D_{32}(initial)}$. This is a dimensionless relation related the time and the Saute mean diameter.

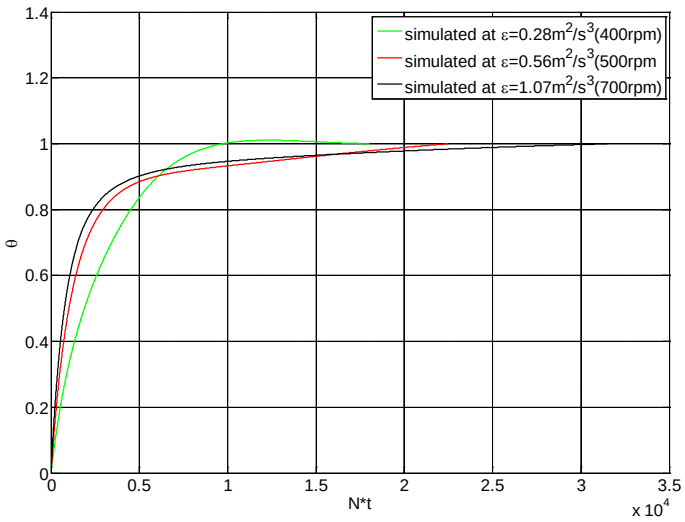

Figure 3.1-11. Master curve for different energy dissipation.

Keeping the parameter σ of the log-normal distribution function unchanged, four different cases of the initial conditions were simulated with impeller speed of 410 rpm where the average energy dissipation rate is 0.307$m^2 \cdot s^{-3}$. The initial $\mathrm{D_{geo}}$ is increased from the 140 μm to 200 μm. The predicated D_{32} of four cases achieved the same steady valves in the end. The final values for D_{32} are 117.1μm, 115.7μm 115.85μm and 117μm corresponding to initial $\mathrm{D_{geo}}$140μm, 160μm 180μm and

200μm respectively. It demonstrated that the initial conditions have no impact on the final steady state. The final droplet size distribution is determined only by the equilibrium between breakage and coalescence rates. The detail about transient D_{32} is shown in Fig. 3.1-12.

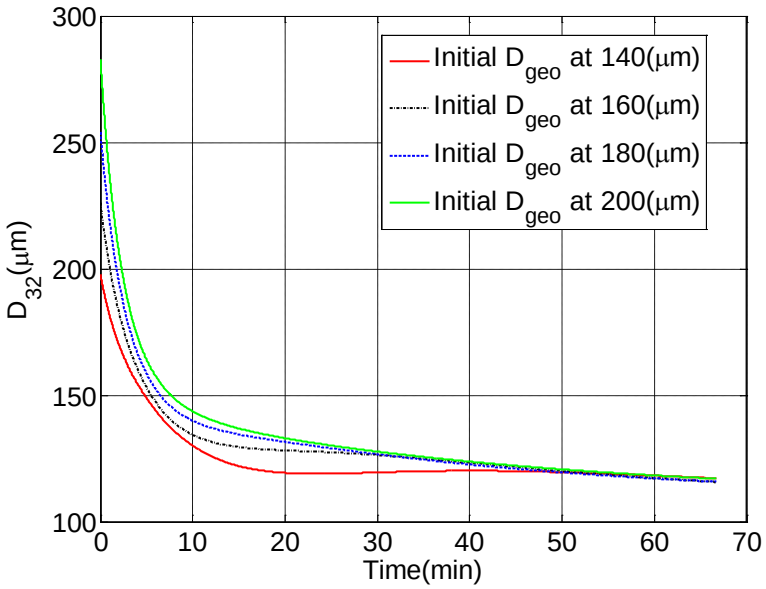

Figure 3.1-12. Evolution of the Sauter mean diameter with different initial conditions.

In this section, the results about the simulation and prediction of D_{32} are analysed by comparison with experimental data. In order to improve the performance of prediction of D_{32}, a new set of parameters is necessary for every different system, because the influence of these factors is not negligible. Although, the accuracy of the predication on D_{32} is not satisfactory, it still demonstrates the correct trend of the transient D_{32}. The energy dissipation rate is a major factor affecting the Sauter mean diameter D_{32}, so a very careful evaluation of power input is key factor to obtain good accuracy.

3.1.5. Conclusion

A breakage-coalescence equation has been derived in a continuous form with droplets length as internal coordinate. Breakage model and coalescence model have been derived to fit into a general PBE. QMOM is introduced as a reliable approach to integral equation providing numerical solution. The results of simulation are compared with the experimental data on aspects of the moments and D_{32} to

demonstrate the validation of the model. The empirical parameters for the model developed by Coulaloglou and Tavlarides (1977) have been optimised by fitting the 0^{th} ~5^{th} moments with the measured data. Then, the model has been employed to predicate the D_{32} with fraction of dispersed phase ranging from 15% to 35%. With higher volume fraction of the dispersed phase, larger size of droplets is expected to obtain at equilibrium state. Impact of the power consumption is also investigated. For higher average energy dissipation rate, the smaller size of droplets are expected to be achieve and it is quicker for the system to get steady state. Different initial conditions are also tested to demonstrate they have no impact on the final droplet size distribution.

All the investigation has been carried out by assuming the tank is fully turbulent and well mixed. Actually, the flow filed in the tank is more complicated than that. It would be necessary to expend and improve the model for modelling an inhomogeneous system in the future work.

Acknowledgements

The authers gratefully acknowledge Professor Chris D. Rielly for his valuable discussions, guidelines and help through the whole project.

Nomenclature

$\mathrm{A}(\mathrm{V}-\mathrm{V}_1,\mathrm{t})$	number fraction for the drops of volume $\mathrm{V}-\mathrm{V}_1$ at time t
$\mathrm{A}(\mathrm{V},\mathrm{t})$	number fraction for the drops of volume V at time t
$\mathrm{C}_1, C_1', \mathrm{C}_2, C_2', \mathrm{C}_3, C_3', \mathrm{C}_4$	experimental constants
d	diameter of the impeller (mm)
$\mathrm{D}_{\max}$	maximum diameter of droplet(m)
D	droplet diameter(m)
D_{32}	Sauter mean diameter(mm)
D_i	abscissas for moments transformation
$\mathrm{f}(\mathrm{D},\mu,\sigma)$	log-normal distribution function

$\mathrm{F}(\mathrm{D_i}, \mathrm{D_j})$	rate of coalescence of droplet of diameter $\mathrm{D_i}$ and $\mathrm{D_j}$
$\mathrm{F}(\sqrt[3]{\mathrm{D}^3 - \mathrm{L}^3}, \mathrm{L})$	coalescence rate between two droplets with diameter $\sqrt[3]{\mathrm{D}^3 - \mathrm{L}^3}$ and L
$\mathrm{g}(\mathrm{L})$	breakage frequency of droplet of diameter L
$\mathrm{g}(\mathrm{V})$	breakage frequency of droplet of volume V
$\mathrm{h}(\mathrm{D}, \mathrm{L})$	coalescence efficiency for droplet with diameter D and L
h_{st}	width of the impeller (mm)
h	distance between the bottom of the tank and the impeller (mm)
H	height of liquid in the tank (mm)
k	numerical constants
l	length of baffle (mm)
L	droplet diameter(m)
$\mathrm{m}(\mathrm{L})$	number of daughter droplet of diameter L
$\mathrm{m}(\mathrm{V_1})$	number of daughter droplet of volume $\mathrm{V_1}$
m_{PVA}	mass of PVA (ug)
m_{H_2O}	mass of water (g)
$\mathrm{n}(\mathrm{L}, \mathrm{t})$	number density of droplets of diameter of L at time t
$\mathrm{n}'(\mathrm{D}^3, \mathrm{t})$	number density of droplets based on volume of D^3at time t
$\mathrm{N}(\mathrm{t})$	total number of droplets at time t
N	number of quadrature points
Ne	power number
N_{speed}	speed of the impeller(rpm)
P	power input(w); matrix for product-algorithm
S_B	width of the baffle(mm)
t	time(s)
T	tank diameter(mm)
V_{tank}	volume of tank(L)
V	volume of droplet(m^3)
$\mathrm{V_1}$	volume of droplet(m^3)

V_{max}	maximum volume of drop(m^3)
w_i	weights from moments transformation
w_j	weights from moments transformation

Greek Symbols

$\beta(D, L)$	frequency of daughter drops of diameter D resulting from breakage of parent drops of diameter L
ε	energy dissipation rate (w/kg)
$\lambda(D, L)$	collision frequency between drops of diameter D and L
μ_k	moments with number k
μ	viscosity $(kg \cdot m^{-1} \cdot s^{-1})$
μ_d	viscosity of dispersed phase$(kg \cdot m^{-1} \cdot s^{-1})$
ρ_{ave}	average density of system $(kg \cdot m^{-3})$
ρ_c	density of continuous phases $(kg \cdot m^{-3})$
ρ_d	density of dispersed phases $(kg \cdot m^{-3})$
σ	interfacial tension $(mN \cdot m^{-1})$
ϕ	volume fraction of dispersed phase over whole volume of system

Referecnces

Alopaeus, V., Koskinen,J., Keskine,K.I., (1999), ”Simulation of the population balances for liquid-liquid system in a nonidela stirred tank. Part 1: Description and qualitative validation of the model”, *Chem. Eng. Sci.*, Vol. 54, pp.5887-5899.

Alopaeus, V., Koskinen,J., Keskine,K.I.,Majander,J., (2002), ”Simulation of the population balances for liquid-liquid system in a nonidela stirred tank. Part 2: Parameter fitting and the use of the multiblock model for dense dispersions”, *Chem. Eng. Sci.*, Vol. 57, pp.1815-1825.

Alopaeus, V., Laakkonen,M., Aittamaa,J. (2006), ”Numercial solution of moments-transformed population balance equation with fixed quadrature points”, *Chem. Eng. Sci.*, Vol. 61, pp.4919-4929.

Andersson, R.& Andersson, B., (2006), “On the breakup of fluid particles in turbulent flows”, American Institute of Chemical Engineering Journal, Vol. 52, pp.2020–2030.

Azizi,F.,& Al Taweel,A.M., (2011), ”Turbulently flowing liquid-liquid dispersion. Part 1:Drop breakage and coalescence”, *Chem. Eng. J.,* Vol. 166, pp.715-725.

Coulaloglou, C. A., & Tavlarides, L.L., (1977), ”Description of interaction processes in agitated liquid-liquid dispersions”, *Chem. Eng. Sci.,* Vol. 32, pp.1289-1297.

Falola, A., Borissova, A., Wang, X. Z., (2013), ”Extended method of moment for general population balance models including size dependent growth rate, aggregation and breakage kernels”, *Computer and Chemical Engineering*., Vol.56,pp.1-11.

Gimbun, J., Rielly, C.D., Nagy, Z.K., (2009), ”Modelling of mass transfer in gas–liquid stirred tanks agitated by a Rushton turbine and CD-6 impeller: a scale-up study”, *Chemical Engineering Research and Design*, Vol. 87,pp. 437–451.

Gordon, R.G., (1968), “Error bounds in equilibrium statistical mechanics”, *Journal of Mathematical Physics*, Vol. 9, pp.655–667.

Hsia, A.M.& Tavlarides, L. L.(1983), “Simulation analysis of drop breakage, coalescence, and micromixing in liquid–liquid stirred tanks”, *Chem. Eng. J.*, Vol. 26, pp.189-199.

Lasheras, J.C.,Eastwood, C., Martinez-bazan, C.& Montanes, J. L., (2002),” A review of statistical models for the break-up of an immiscible fluid immersed into a fully developed turbulent flow”, *International Journal of Multiphas Flow*, Vol. 28, pp.247-278.

Lee, C.H., Erickson, L.E., Glasgow, L.A., (1987),'' Dynamics of bubble size distribution in turbulent gas–liquid dispersions'', *Chem. Eng.Commun*. Vol.61,181-195.

Luo, H.& Svendsen, F., (1996), “Theoretical model for drop and bubble break-up in turbulent dispersions”, *AIChE J.,* Vol. 42, pp.1225-1233.

Marchisio, D.L.& Fox,R.O., (2005), ”Solution of population balance equation using the direct quadrature method of moments”, *Aerosol Science,* Vol. 36,pp.43-73.

Marchisio, D.L.,Vigil, R.D., Fox, R.O., (2003a), ”Quadrature method of moments for aggregation-breakage processes”, *Journal of Colloid and Interface Science*, Vol. 258, pp.322-334.

Marchisio, D. L., Pikturna, J., Fox, R. O., Vigil, R. D., & Barresi, (2003b), ”Implementation of the quadrature method of moments in CFD codes for aggregation-breakage problems”, *Chem. Eng. Sci*., Vol. 58(15), pp.3337-3351.

Marchetti, J.M. & Svendsen H.F.(2012), “Review of kernels for droplet-droplet interaction droplet-wall collision, entrainment, re-entrainment and breakage”, *Chem. Eng. Comm*. Vol. 199, pp.551-575.

McGraw,R.(1997),”Description of aerosol dynamics by the quadrature method of moments”, *Aerosol Science and Technology,* Vol. 27, 255–265.

Maab, S.Metz, F., Rehm, T. Kraume, M. (2010), ’’Prediction of drop sizes for liquid-liquid systems in stirred slim reactors-Part 1: single stage impellers’’, *Chem. Eng. J.,* Vol. 162, pp792-801.

Prince, M.J.& Blanch, H.W.(1990), ”Bubble coalescence and break-up in air-sparged bubble columns”, *AIChE J., Vol.* 36, pp.1485-1499.

Randolph,A.D. & Larson, M.A.(1971).’’ Theory of particulate process: analysis and techniques of continuous crystallisation’’, New Tork:academic press.

Valentas, K. J., Bilous, O., & Amundson, N. R., (1966), ”Analysis of breakage in dispersed phase systems”, *Ind.Eng. Chem. Fundam*., Vol 5, pp.271-279.

Chapter 4

4.1. Conclusion and Recommendations

Although the simulated results showed good agreement on the moments, the predicated Sauter mean diameter does not offer satisfying agreement with measured data. It is believed that the program code still needs to be further refinement, especially for inputting physical parameters and generating the original data of moments.

The physical parameters are regarded as constant incorporated into the equation. It would be better that they can be changed into the form of the variables so that the model can be modified and applied into more specific system. As the current moments are all analysed with normalising by the 0^{th} moment, it would be interesting to identify the performance of the moments without normalising.

The influence of geometric set-up of the tank also needs to be investigated such as the ratio of the liquid height and vessel diameter, type of the impeller, numbers of the impeller and baffles.

The average energy dissipation rate is the main source for the errors in the current work, to improve the accuracy, the varied energy dissipation rate with different spatial position was suggested to investigate in the future work. If possible, an experimental rig about the liquid-liquid mixing is also expected to set up.

.

4.2. Appendices

4.2.1. MSc Project Plan

Project Introduction and Plan

This project is to model the process of immiscible dispersion of one liquid in another within a stirred vessel by using methods such as the population balance equations. When two mutually insoluble liquids are mixed in a vessel, an immiscible liquid-liquid system is formed, for instance, a dispersion containing oil and water. Initially, the droplets are not stable and will be deformed with time through two ways, break-up or coalescence. The droplet size distribution is commonly used to describe the system at a certain time. To control the rate of break-up and rate of coalescence, surfactant, and suspension agent are added into the system. An agitator is also used to control the process by changing the physical properties such as speed or size of impellers. After a while, the size of droplets will reach a dynamic equilibrium. The purpose of this project is to identify the time that is required to reach the equilibrium state by establishing a proper population balance model. A population balance model includes many sub-models for phenomena such as breakage rate, coalescence rate daughter sizes. Considering influences of different kinetics kernels for a specific system, an appropriate population balance equation will be constructed. Then, some real experimental data will be fit into the equation to test the validation of the model Most information will be from the report done by Sebastian Maab(2010) . If the error is within the range that can be accepted, the equation is applied into the predication of the system and modifying through the new data. It will be repeated till proper parameters are found. This project involves large amount of calculation, so the software like MATLAB will be used.

Aims and Objectives:

- Review literature about population balance modelling of immiscible liquid-liquid system.
- Finish a preliminary Literature survey about PBE, maximum 2500 words

- Population balance equation need to be solved by choosing appropriate method such as quadrature method of moments with proper program in MATLAB.
- Choose an appropriate style of a journal article and finish an interim report.
- Optimise the models by using measured data or comparison with others' literature
- Write a manuscript based on the investigation, no more than 5000 words

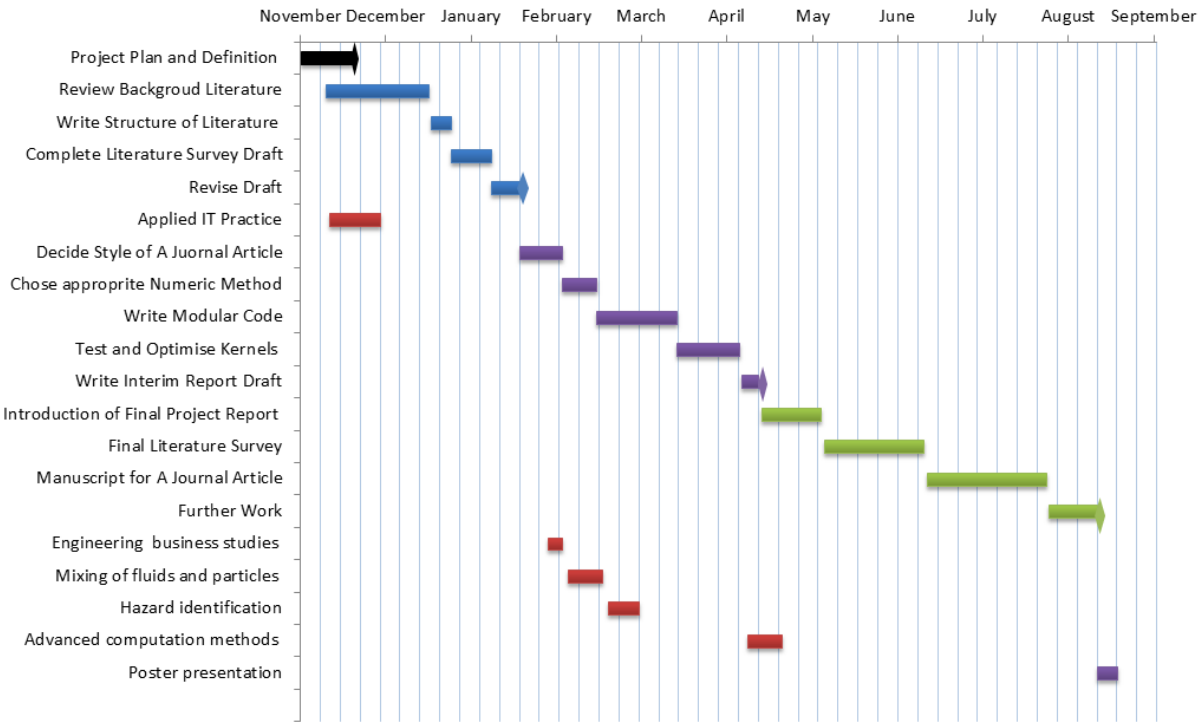

4.2.2. Meeting Minutes

1. Meeting date: 17/10/2012

2. Meeting location: Room S.2.39

3. Items for discussion

   - The introduction of immiscible liquid-liquid system
     When two insoluble liquids are mixed in a stirred tank, for example, oil and water, the liquids are present as separate phases at first. After a while, the phases can turn into the dispersed phase and the continuous phase. During this process, different size of droplet is formed through dispersion or coalescence. We mainly focus on the distribution of size of droplet.

   - The Drop Size Distribution(DSD)
     A normal distribution is used to describe the probability density. The mean diameter of drop and the breadth of curve are varied with time. Breakage and coalescence are two different types used to describe the deformation of droplets.

   - General process to identify a liquid-liquid system
     Build population balance models; quantify the models by doing experiment; find the parameters that affect the models; predict a new liquid-liquid system.

   - Hand Book of Industrial Mixing(chapter 12)
     Edward L Paul; Suzanne M Kresta; Victor A Atiemo-Obeng; North American Mixing Forum, c2004.

4. Next meeting: 24/10/2012 4.00pm

1. Meeting date: 24/10/2012

2. Meeting location: Room S.2.39

3. Items for discussion

- The role of surfactant
  Surfactant consists of two parts: hydrophobic group and hydrophilic group. The hydrophobic group can be integrated into an oil particle, while the hydrophilic group is still on the surface of the oil particle which reduces the possibility of the particle to coalesce with the other oil particle which also adhered by surfactants.

- The terms that used to describe the DSD
  Sauter mean diameter which is the ratio of the average drop volume and the average drop surface.
  $$\boldsymbol{D_{32} = \frac{\sum D_i^3}{\sum D_i^2} = \frac{\mu_3}{\mu_2}}$$
  Where $\boldsymbol{\mu_3 = \int_o^\infty D^3 P_x(D) dD}$ $\boldsymbol{\mu_2 = \int_0^\infty D^2 P_x(D) dD}$

- The definition of dispersed phase concentration
  The dispersed phase concentration is usually expressed as a volume fraction.
  $$\emptyset = \frac{\boldsymbol{volume\ of\ oil}}{\boldsymbol{volume\ of\ oil\ and\ water}}$$

- Techniques used to observe flow of droplets in a turbulent stirred tank.
  LDV (laser Doppler velocity)
  PIV (particle image velocimetry)

- Capillary number and viscosity ratio
  $$Ca = \frac{\mu_c G\ a}{\sigma}$$
  Where a is viscosity ratio and G is the stain rate/ deformation rate

4. Next meeting: 31/10/2012 10.30am

1. Meeting date: 31/10/2012

2. Meeting location: Room S.2.39

3. Items from last meeting

- The role of surfactant
  Surfactant consists of two parts: hydrophobic group and hydrophilic group. The hydrophobic group can be integrated into an oil particle, while the hydrophilic group is still on the surface of the oil particle which reduces the possibility of the particle to coalesce with the other oil particle which also adhered by surfactants.

- The terms that used to describe the DSD
  Sauter mean diameter which is the ratio of the average drop volume and the average drop surface.
  $$\boldsymbol{D_{32} = \frac{\sum D_i^3}{\sum D_i^2} = \frac{\mu_3}{\mu_2}}$$
  Where $\boldsymbol{\mu_3 = \int_o^\infty D^3 P_x(D) dD}$ $\boldsymbol{\mu_2 = \int_0^\infty D^2 P_x(D) dD}$

- The definition of dispersed phase concentration
  The dispersed phase concentration is usually expressed as a volume fraction.
  $$\emptyset = \frac{\boldsymbol{volume\ of\ oil}}{\boldsymbol{volume\ of\ oil\ and\ water}}$$

- Techniques used to observe flow of droplets in a turbulent stirred tank.
  LDV (laser Doppler velocity)
  PIV (particle image velocimetry)

- Capillary number and viscosity ratio
  $$Ca = \frac{\mu_c G\ a}{\sigma}$$
  Where a is viscosity ratio and G is the stain rate/ deformation rate

4. Items for next meeting

5. Next meeting: 2/11/2012 10.30am

1. Meeting date: 2/11/2012

2. Meeting location: Room S.2.39

3. Items from last meeting

- The relationship between D_{32} and D_{max}
  If the turbulent system is geometrically similar, we can assume that the D_{max} is proportional to D_{32}. This relationship can be written as follow:

$$\frac{d_{32}}{D} = C_2 * We^{-\frac{3}{5}}$$

- Equilibrium drop size distribution and extension to other devices
  Since the factors such as impeller design, impurities presence of surfactants or suspending agents and local energy dissipation etc., it is very complex to estimate the mean drop size and distribution. Therefore several different equations have been developed for every single case.

- Time to equilibrium and transient drop size in turbulent flow
  The time that uses to reach equilibrium can be described as follow:

$$\frac{d\Omega}{d\theta} = -\alpha_1 \Omega^{\alpha_2}$$

  Where $\Omega = \frac{d_{32}(t) - d_{32}^{\infty}}{d_{32}^{\infty}}$ and $\theta = Nt$

4. Items for next meeting
   - Population Balance Modelling
   - Drop coalescence

5. Next meeting: 9/11/2012 4.00pm

1. Meeting date: 09/11/2012

2. Meeting location: Room S.2.39

3. Items from last meeting

   - Basic principles of drop coalescence
     Coalescence efficiency which depends on hydrodynamic factors is probability of coalescence per collision.
     Coalescence frequency is collision rate.

   - Factors influencing coalescence
     The condition of the interface is between a rigid interface and mobile interface has an effect on film drainage time.
     Viscosity of drop, interfacial tension, collision forces, surfactants and impurities are also factors influencing film drainage time.

   - According to the time for dispersion to separate, immiscible liquid-liquid systems can be characterized into several different types.

   - Introduction of population balances modelling
     To simplify the general population balance equation, moments are introduced, and lower order moments, which can be related to number, surface, volume or weight, are investigated.

4. Items for next meeting
   - Further discussion on Population Balance Modelling

5. Next meeting: 16/11/2012 4.00pm

1. Meeting date: 11/03/2013

2. Meeting location: Room S.2.39

3. Items from last meeting

   - Feedback of literature review
     All symbols and letters should be explained in the nomenclature.
     Keep form of formulas consistent.

     It should contain more critical thinking.

     A solution should be provided

   - Decide a method for solving PBE
     Two methods that could be used to solve the PBE are: 1) discretized droplets distribution;2) Quadrature method of moments.
     It is more likely to use QMOM, as it is more practical and easier and detail of QMOM is possible to be found from work of Marchisio.

   - MATLAB
     Learn it by relevant sources on websites or books
     Send Yang an example of Matlab code

4. Items for next meeting
   - Further discussion on method used to solve PBE

5. Next meeting: 19/03/2013 2.00pm